The obesogenic potential of high fat/high protein diets is determined by both amino acid- and fatty acid composition of the protein source used

KARIANNE KORSMO

MASTER THESIS IN HUMAN NUTRITION

DEPARTMENT OF CLINICAL MEDICINE

FACULTY OF MEDICINE AND DENTISTRY, UNIVERSITY OF BERGEN

MAY 2016

The obesogenic potential of high fat/high protein diets is determined by both amino acid- and fatty acid composition of the protein source used

MASTER THESIS IN HUMAN NUTRITION

KARIANNE KORSMO

MAY 2016

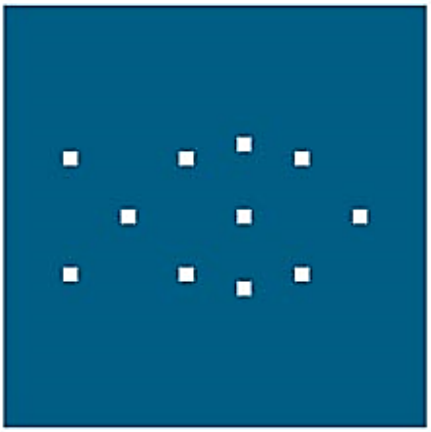

N I F E S

NATIONAL INSTITUTE
OF NUTRITION AND
SEAFOOD RESEARCH

ACKNOWLEDGEMENTS

The work presented in this thesis was performed at the National Institute of Nutrition and Seafood Research (NIFES) in Bergen from autumn 2015 to spring 2016.

First, I would like to thank my main supervisor Dr. Philos Even Fjære for introducing me to the interesting field of nutritional research, for his guidance and optimism throughout the year and for always making the time to answer my numerous questions. Further, I would like to thank my co-supervisor Dr. Philos Lise Madsen for encouragement and advice along the way and my co-supervisor Dr. Philos Livar Frøyland for reviewing my thesis and giving me useful and positive feedback.

I would also like to thank Dr. Philos Lene Secher Myrmel for her help with animal testing and handling data from qPCR and for always making herself available for assistance. A thank you also goes to Astrid Elise Hasselberg for her superb assistance with animal care and valuable tutoring along the way.

Additionally, I would like to express my gratitude to Hui-Shan Tung, Synnøve Wintertun and Eva Mykkeltvedt for teaching me RT-qPCR. A thank you also goes to the Molecular Imaging Center at Haukeland University Hospital for conducting sectioning of my histology samples.

To my fellow master students I would like to say thank you for lots of laughter and support. Especially thanks to Anita for great cooperation with the animal experiment and for always solving my IT-problems.

The final thanks goes to than Hans Petter for his great patience and for crucial support, comfort and motivation through the entire year.

Bergen, May 2016
Karianne Korsmo

TABLE OF CONTENTS

LIST OF FIGURES

Appendix

LIST OF TABLES

Appendix

LIST OF ABBERIVATIONS

2-AG: 2-arachidonoylglycerol
AA: Arachidonic acid
ABC: Avidin-biotin-peroxidase-complex
AEA: Anandamide
ALA: α-linolenic acid
ANOVA: Analysis of variance
AOC: Area over the curve
ATP: Adenosine-5'-trifosfat
AUC: Area under the curve
BAT: Brown adipose tissue
BCAA: Branched-chain amino acids
BMI: Body mass index
cAMP: Cyclic-adenosine monophosphate
CB1: Cannabinoid receptor-1
CB2: Cannabinoid receptor-2
CVD: Cardiovascular disease
DAB: Diaminobenzidin tetrahydrochloride
DHA: Docosahexaenoic acid
E%: % of total energy
EC: Endocannabinoid
ECS: The endocannabinoid system
EPA: Eicosapentaenoic acid
EtOH: Ethanol
eWAT: Epididymal white adipose tissue
FA: Fatty acid
FFA: Free fatty acid
H&E: Hematoxylin and eosin
HF: High fat
HF/HP: High fat/high protein
HF/HS: High fat/high sugar
HP: High protein
IL-6: Interleukin-6
iBAT: Interscapular brown adipose tissue
ITT: Insulin tolerance test
iWAT: Inguinal white adipose tissue
LA: Linoleic acid
LF: Low fat
MetOH: Methanol
MRI: Magnetic resonance imaging
n-3: Omega-3
n-6: Omega-6
OGTT: Oral glucose tolerance test
qPCR: quantitative real-time polymerase chain reaction
PB: Phosphate buffer
PBS: Phosphate-buffered saline
PKA: Protein kinase A
PUFA: Polyunsaturated fatty acid
RM: Repeated measurements
RT: Reverse transcription
rWAT: Retroperitoneal white adipose tissue
TG: Triacylglycerol
TNF-α: Tumor necrosis factor-α
UCP1: Uncoupling protein-1
WAT: White adipose tissue
WHO: World Health Organization

ABSTRACT

Background: Studies in rodents have found that high protein diets differ in obesogenic potential depending on the protein source used. Varied changes in morphology of brown adipose tissue, an important metabolic organ in mice and rats, have also been observed. Whether diversity in obesogenic potential of different protein sources is caused by amino acid composition, fatty acid composition or a combination of both is unknown. Further, little is known about causes and consequences of changes in brown adipose tissue morphology.
Methods: Male C57BL/6J BomTac mice were fed different high-fat/high-protein diets. Casein, cod, pangasius and chicken was used as protein sources, but they also provided different amounts and types of fat to the diet. Pangasius, high in omega-6 fatty acids and with similar amino acid composition as cod, was used to distinguish between the effect of amino acid- and fatty acid composition. Four groups were fed *ad libitum*, and one group was fed restricted amounts of the chicken-based diet in order to evaluate the impact of weight gain on brown adipose tissue activity and morphology. We studied the effect of different protein sources on body weight development, energy intake, body composition, glucose homeostasis and gene expression in interscapular brown adipose tissue. Body composition was determined by MRI-scan and histology was carried out to examine changes in adipose tissue morphology. Insulin tolerance test and oral glucose tolerance test were performed to assess insulin sensitivity and glucose tolerance. Uncoupling protein-1 (UCP1) expression in brown adipose tissue (BAT) was analyzed by real time-qPCR and immunohistochemistry.
Results: A high-fat/high-protein diet based on chicken was obesogenic relative to the one based on cod, whereas the pangasius-based diet had an intermediate effect. Calorie restriction attenuated changes in BAT morphology caused by the chicken-based diet. Similar classic BAT morphology as the one observed in lean chicken-fed mice was also observed in mice fed casein and pangasius. Little differences was observed in gene expression, but immunohistochemistry revealed higher expression of UCP1 in mice fed casein, pangasius and chicken in restricted amounts.
Conclusion: Both amino acid- and fatty acid composition determines the obesogenic potential of different protein sources in high-fat/high-protein diets. Changes in BAT morphology and activity are partially decided by body weight, but pangasius as protein- and fat source attenuates this effect. Mice fed casein remains lean with a classic BAT morphology.

1.0 Introduction

1. 1 Overweight and obesity

Overweight and obesity are one of the biggest health concerns worldwide. In 2014, about 39 % of the world's adult population (18 ≤ years) were overweight. This equals more than 1,9 billion people. Of these, over 600 million, 13 % of the adult population, were obese (WHO 2015). Alarmingly, the prevalence of obesity amongst children is also on the rise. Overweight among children under the age of five has increased from 4,8 % in 1990 to 6,1 % in 2014. The greatest increase has happened in low- and middle-income countries (WHO 2016).

Overweight and obesity are defined as abnormal or excessive fat accumulation that may impair health (WHO 2015). Body weight index (BMI) is the most common measurement used to classify these conditions. The definition of BMI is a person's weight (kg) divided by the persons square of height (m^2). WHO's definition of overweight and obesity are as follows (WHO 2015):

- BMI ≤ 25 = overweight
- BMI ≤ 30 = obesity class I
- BMI ≤ 35 = obesity class II
- BMI ≤ 40 = obesity class III

It is important to notice that BMI is a valuable way of measuring overweight and obesity on population level. It is, however, an unsatisfying estimate on an individual level due to the lack of information on body composition and fat distribution (Bere 2011).

1.1.1 Causes

The causes of overweight and obesity are both intricate and diverse. A positive energy balance has traditionally been considered as the fundamental cause, which means that consumption of calories is in excess of calories used (WHO 2015). This may be caused by increased consumption, less physical activity or a combination of both. If this is the case, then the resolution to prevent and avoid overweight and obesity is a restricted calorie intake and/or increasing the physical activity level. However, this "calories in = calories out" theory is now under debate (Williams et al. 2015, Lucan and DiNicolantonio 2015). It may be that calories from fat, protein and carbohydrate have a different impact on weight gain (van Dam and Seidell 2007, Leidy et al. 2007). If this is the case, than the diet's macronutrient composition

is also a determining factor for developing overweight. Today's increasing intake of processed food containing high amounts of salt, omega-6 fatty acids (FAs) and refined carbohydrates might lead to a less profitable composition (FAO 2013).

A more sedentary lifestyle with less physical activity is also a factor contributing to the increased prevalence of overweight and obesity (WHO 2015), as well as genetic factors (O'Rahilly and Farooqi 2000). Novel research on gut microbes, microbiota, has highlighted yet another possible cause (Ley et al. 2006).

1.1.2 Health consequences

Overweight and obesity are associated with increased risk of a number of noncommunicable diseases:

- Cardiovascular diseases (CVDs) such as hypertension, atherosclerosis, heart failure and stroke
- Insulin resistance and type 2 diabetes
- Some types of cancer
- Osteoarthritis

It may also have psychological consequences such as depression, body dissatisfaction, bulimia and low self-esteem (Kyrou, Randeva, and Weickert 2000).

1.1.3 High protein- and high fat diets

Fat is the most energy dense macronutrient (9 kcal/g), and so a low fat (LF) diet has traditionally been viewed as the best way of weight reduction and weight management (Helsedirektoratet 2014). The validity of the "calories in = calories out" theory is now under debate and as a result, diets that focus on macronutrient distribution rather than calorie intake has become increasingly popular. Intake of carbohydrates leads to insulin secretion and insulin induce lipogenesis and glycolysis. High fat (HF) diets, replacing carbohydrates with fat to reduce insulin secretion, is one way of changing the macronutrient distribution of the diet (Taubes 2010). Given the elevated diet-induced thermogenesis from protein (20 -30 %) compared to carbohydrates (5-10 %) and fat (0-3 %) (Tappy 1996), high protein (HP) diets have also gained more interest. HP diets are also thought to have a high satiating effect (Westerterp-Plantenga, Lemmens, and Westerterp 2012). Studies have found that high protein

diets attenuates obesity in rodents. However, most of these studies uses diets based on milk protein such as whey or casein, whereas humans usually eats fish and meat as well (Liisberg, Myrmel, et al. 2016). Studies investigating the effect of HP diets in humans are not consistent (Te Morenga and Mann 2012, Halton and Hu 2004). Different protein sources may vary in obesogenic potential (Gilbert et al. 2011), and further investigation on the effect of different HP diets could therefore be of interest.

1.2 Omega-6 and omega-3 essential fatty acids

Omega-6 and omega-3 FAs are two classes of polyunsaturated fatty acids (PUFAs). The position of the first double bond, counting from the methyl end of the FA, is what generated the two names. In the n-6 and n-3 FAs, this bond is located at C-6 and C-3 respectively. The n-6 FA linoleic acid (LA, C18:2) and the n-3 FA α-linolenic acid (ALA, C18:3) are both essential fatty acids and crucial components of a healthy diet. However, the metabolism of LA and ALA to their higher unsaturated derivatives, arachidonic acid (AA, C20:4n6) and eicosapentaenoic acid (EPA, 20:5n3)/docosahexaenoic acid (DHA, 22:6n3), relies partially on the same enzymes (Figure 1.1). This leads to a competition between LA and ALA where high amounts of either FA might suppress the metabolism of the other. A balanced intake is therefore of importance (Russo 2009).

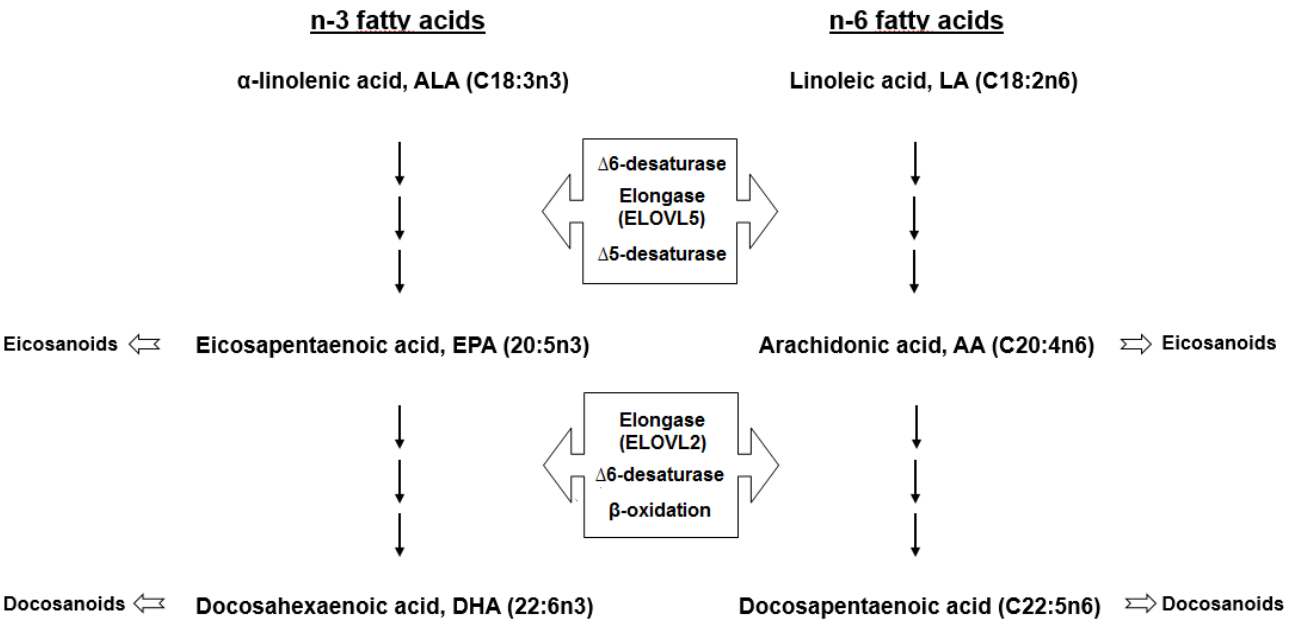

Figure 1.1 Metabolism of essential fatty acids. ALA and LA competes for the same enzymes towards the production of their 20- and 22-carbon derivatives. EPA and AA are precursors of eicosanoids and DHA for docosanoids.

Following synthesis, AA and EPA/DHA are included in tissue membranes, thus affecting the fluidity of the membranes. This will further influence the activities of membrane-bound proteins. Once incorporated in cell membranes, EPA and AA also act as substrates for eicosanoid synthesis. Eicosanoids are a family of signaling molecules that includes prostaglandins, thromboxanes, leukotrienes, endocannabenoids among others. In general, eicosanoids derived from AA endorse a pro-inflammatory state, whereas those synthesized from EPA countervail this effect (Harris 2006).

1.2.1 Changes in consumption of omega-6 and omega-3 and possible consequences

Today's diet is widely different from our ancestor's hunter-gatherer diet. Early man ate a diet based on uncultivated fruits and vegetables, seeds, nuts and wild game. The consumption of cereal grains where little to none. In today's diet, cereal grains such as wheat, maize and rice account for a large amount of energy consumed (Simopoulos 2002). Furthermore, there is an increasing intake of vegetable oil such as soybean oil and canola oil. From year 1909-2000, consumption of vegetable-, salad- and cooking oils in the U.S. went from almost zero to near

18 kg per capita per year (Gerrior 2004). Additionally, wild game has been replaced with grain-fed livestock. One consequence of these changes is an increased intake of n-6 FAs and a change in the dietary n-6/n-3-ratio from ~1 to 15/1-16/1 (Simopoulos 2002).

A high intake of LA might lead to a decreased tissue concentration of EPA and DHA. Furthermore, it may also engender increased concentrations of LA- and AA-phospholipids in cell membranes (Blasbalg et al. 2011, Alvheim et al. 2012). Considering the fact that n-6 eicosanoids in general endorse inflammation, this may promote a prothrombotic and proaggregatory physiological state (Simopoulos 1999). Alvheim et.al (Alvheim et al. 2012) found that increasing dietary LA contributed to increased prevalence of obesity in mice. An increased consumption of LA, and the primary dietary sources of this FA, were also positively correlated with greater risk of obesity in humans. Further, the high intake of n-6 FAs in Western countries today is associated with the persistently high rate of CVD and the incidence of certain cancers (de Lorgeril and Salen 2012).

The relationship between n-6 fatty acids, inflammation and CVD is, however, a matter of debate. A systematic review of 15 randomized controlled trials found virtually no evidence that an increased intake of LA leads to higher concentration of inflammatory markers (Johnson and Fritsche 2012). Harris et.al (Harris, Assaad, and Poston 2006) pooled data from case-control and prospective cohort studies, and found no evidence of adverse effects of n-6 FAs on CVD.

Due to these inconsistent results, the use of the n-6/n-3 ratio as a target for reducing inflammation and risk for CVD has been criticized (Harris 2006). There is evidence that an increased intake of n-3 FAs, which will give a lower n-6/n-3 ratio, will reduce the risk of CVD (FAO 2010). However, the evidence regarding the intake of n-6 intake and CVD are inconsistent, even though a reduction of n-6 FAs will have the same effect on the n-6/n-3 ratio. It might be more expedient to focus on the absolute amounts of n-3 and n-6 FAs, rather than the ratio. For instance, the conversion of ALA to its higher unsaturated derivatives seems to be determined by the amounts of ALA and LA in the diet, not the ratio (Goyens et al. 2006).

1.2.2 The endocannabinoid system

The endocannabinoid system (ECS) consists of the endocannabinoids (ECs), the proteins catalyzing their biosynthesis and inactivation as well as the cannabinoid receptors. In the mid-1960's, the chemical structure of tetrahydrocannabinol, the major psychoactive component of the cannabis plant, were discovered. Further studies revealed that this component works by binding to specific plasma proteins and two cannabinoid receptor subtypes were identified: Cannabinoid receptor-1 (CB1) and cannabinoid receptor-2 (CB2). The discoveries of these receptors further led to the search for endogenous ligands, endocannabinoids, capable of activating them. Anandamide (N- arachidonoylethanolamine; AEA) was the first to be identified, followed by 2-AG (2-arachidonoylglycerol). These are still the most studied endocannabinoids and together with all others, they derive from AA-containing phospholipids. The ESC are thought to participate in a wide variety of responses, including control of food intake, energy expenditure, and glucose homeostasis (Matias and Di Marzo 2007). CB1 is expressed in the brain, the gastrointestinal tract, skeletal muscle and adipose tissue, underlining the fact that the ESC regulates food intake and energy metabolism both at a central and peripheral level (Kim, Li, and Watkins 2011).

As the endocannabinoids derives from a n-6 FA, it has been suggested that changes in the dietary n-6/n-3 ratio might affect ECS-activity (Simopoulos 2016). A study by Alvheim et al. (Alvheim et al. 2012) showed that increased amounts of LA in the diet led to increased AA content in red blood cell phospholipids. This was seen together with elevated levels of 2-AG and AEA in liver (Alvheim et al. 2012). Increased levels of endocannabinoids can further lead to increased appetite and food intake (Kirkham et al. 2002). Moreover, an increased intake of n-3 FAs seems to lower levels of AA in membrane phospholipids, thereby decreasing the synthesis of anandamide and 2-AG (Alvheim et al. 2012).

1.3 The adipose tissue

There are two different kinds of adipose tissue: White adipose tissue (WAT) and brown adipose tissue (BAT). These consist mainly of white adipocytes and brown adipocytes respectively. The white adipocytes serve as a lipid storage, whereas brown adipocytes are able to burn energy and produce heat (Cinti 2009). Therefore, obesity development may cause changes in the adipose tissue and changes in the adipose tissue may contribute to obesity development.

1.3.1 White adipose tissue

White adipocytes are the major component in WAT. These adipocytes are spherical cells containing a single lipid droplet (unilocular cells). Their size is mainly decided by the extent of this droplet, which constitutes >90% of the cell's volume. The droplet serves as a storage of lipids in the form of triacylglycerols (TGs) (Cinti 2009). Traditionally, WAT has been considered only a storage of energy in the form of fat. However, it is now well established that white adipose tissue is an important endocrine organ, which synthetize and secrete a number of different cytokines, hormones, extracellular matrix proteins and vasoactive factors, all referred to as adipokines. Examples of adipokines are leptin, tumor necrosis factor-α (TNF-α), interleukin-6 (IL-6), etc. (Fruhbeck et al. 2001).

1.3.2 Brown adipose tissue

In contrast to the unilocular white adipocytes, brown adipocytes are multilocular cells containing several smaller lipid droplets. These cells also contains a considerable amount of mitochondria where uncoupling protein-1 (UCP1) is present. UCP1 is a mitochondrial protein that induces heat production, which is the main function of brown adipocytes. They can also act like a fat storage and endocrine cells, but to a lesser extent than that of white adipocytes (Rodriguez et al. 2015).

UCP1 is a transmembrane protein located in the inner mitochondrial membrane. It creates a proton leak across this membrane, thus uncoupling adenosine-5'-trifosfat (ATP) synthesis from the oxidative phosphorylation, and heat is produced. This kind of heat production is called non-shivering thermogenesis. The sympathetic nervous system regulates non-shivering

thermogenesis in BAT. It releases norepinephrine, which binds to β-adrenergic receptors in brown adipocytes. This leads to activation of protein kinase A (PKA) via adenyl cyclase and conversion of ATP to cyclic-adenosine monophosphate (cAMP). PKA further activates triacylglycerol lipase by phosphorylation, which then cleave TGs into free fatty acids (FFAs). The FFAs override the inhibition on UCP1 caused by purine nucleotides leaving the protein active (Cannon and Nedergaard 2004). In rodents, non-shivering thermogenesis is activated when temperature drop below thermoneutrality (28-30 ^{0}C) (Cinti 2009).

In obese animals, the characteristics of the brown adipocytes gradually change to be more like those of white adipocytes. The many small lipid droplets merge into larger ones and the number of mitochondria declines (Cinti 2009).

1.3.3 Beige adipocytes – a third type of fat cell

The major white and brown fat depots are located at anatomically different positions, but as early as the 1980's it was reported that multilocular UCP1-expressing cells could be found within the white adipose tissue after cold exposure (Young, Arch, and Ashwell 1984, Loncar, Afzelius, and Cannon 1988). These cells have later been named beige or "brite" (brown in white) adipocytes. The beige adipocytes are similar to white adipocytes when unstimulated, but cold exposure leads to a change in UCP1 expression making the cells more similar to brown adipocytes. When stimulated, UCP1 expression and non-shivering thermogenesis in beige adipocytes could equal that of brown adipocytes (Peirce, Carobbio, and Vidal-Puig 2014). Studies investigating brite adipocytes have demonstrated that these cells have distinctive gene expression signature, leading to the suggestion that beige adipocytes are a distinct type of fat cells (Wu et al. 2012).

Brown adipocytes derives from the same *Myf5*$^{+}$precursor cell lineage as skeletal muscle cells (Figure 1.2). Transcriptional regulator PRDM16 plays a critical role in the fat/skeletal muscle switch. Binding of this transcriptional regulator to transcription factor PPAR-γ induces differentiation into brown adipocytes in lieu of myocytes (Seale et al. 2008). The cold induced co-activator PGC-1α is also an important regulator of BAT development and function. Binding of PGC-1α to PPAR-γ potentiates UCP1 expression in the adipocyte.

1.3.4 Origin of adipocytes

Until recently, it has been approved that white adipocytes are derived from *Myf5*$^{-}$ precursor cells only (Wu, Cohen, and Spiegelman 2013). However, this view was recently challenged by Sanchez-Gurmaches et al. (Sanchez-Gurmaches et al. 2012), who discovered the presence of some *Myf5*$^{+}$ adipocyte precursors in WAT. Beige adipocytes can derive from white adipocyte precursors, which means that they most likely shares the same *Myf5*$^{-}$ lineage of origin (Wu et al. 2012). It seems like different types of white adipocyte precursors may have a different potential to produce beige adipocytes and that some also are distinct beige precursors (Peirce, Carobbio, and Vidal-Puig 2014). Additionally, studies have indicated that the beige adipocytes can originate directly from mature white adipocytes (Rosenwald et al. 2013, Himms-Hagen et al. 2000) (figure 1.2). However, other studies have found conflicting results (Wang et al. 2013), leaving this interconversion from white to beige an unresolved question.

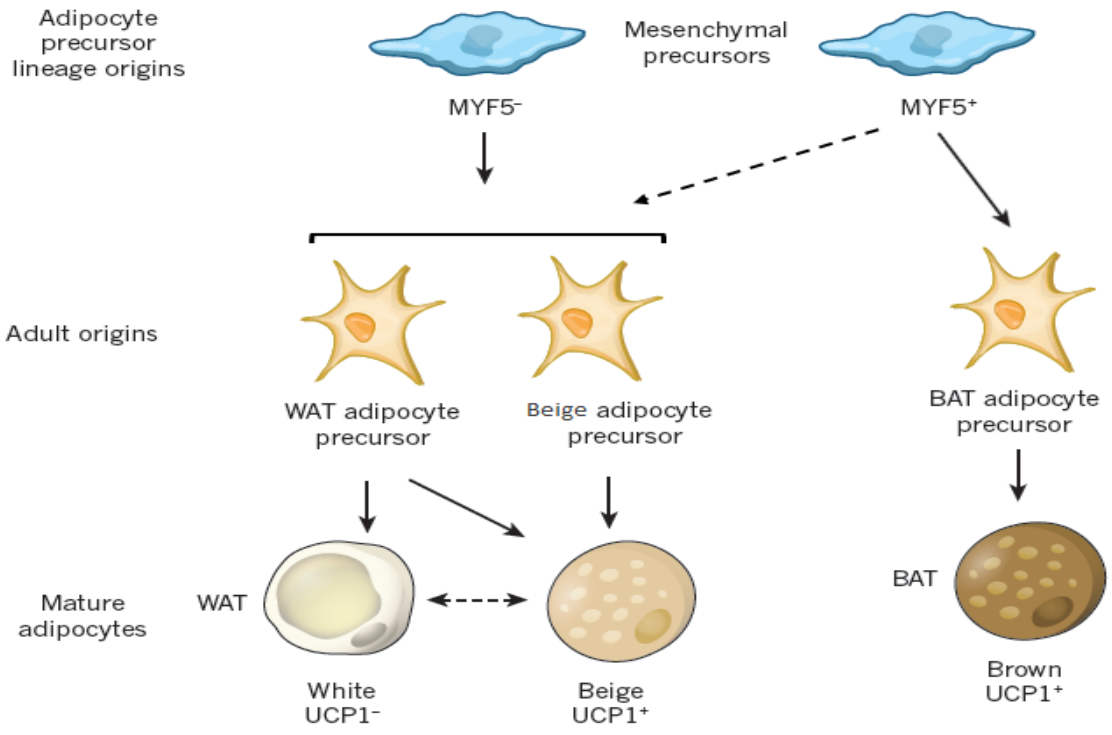

Figure 1.2 Origins of adipocytes. Origin of brown, white and beige adipocytes. Brown adipocytes originates from at *Myf5*$^{+}$ lineage, whereas white and beige originates from *Myf5*$^{-}$ precursors. They may also derive from the same *Myf5*$^{+}$ lineage as brown adipocytes. Figure is adapted from (Peirce, Carobbio, and Vidal-Puig 2014).

The determination of phenotype during adipogenesis seems to involve both transcriptional factors, co-activators and miRNAs as well as epigenetics. PPAR-γ along with its co-activators PGC-1α, SRC1 and PRDM16 appears to promote brown/beige adipogenesis. PGC-1α is an important regulator of the expression of thermogenic genes in brown adipocytes, but it is also an essential regulator of various processes in other cells and organs. Per contra, PRDM16 seem to be more specific at inducing the expression of these genes.

1.3.5 Brown adipose tissue as a target of obesity prevention

BAT is found in mammalians only (Cannon and Nedergaard 2004). In most rodents, it is located both subcutaneously (interscapular, axillary and cervical) and visceral (mediastinal and perirenal) (Cinti 2009). It is also well known that human infants have relatively large active interscapular depots of BAT. In human adults on the other hand, BAT has been thought to be nonfunctional and with no significant physiological relevance (Cannon and Nedergaard 2004). However, recent studies have confirmed that this is not the case (Virtanen et al. 2009, Cypess et al. 2009). This knowledge, combined with the new evidence of beige adipocytes, has revealed a new target of obesity prevention. Both increased activation of existing BAT and induced formation of beige adipocytes in WAT could potentially inhibit excessive weight gain and development of metabolic syndrome (Peirce, Carobbio, and Vidal-Puig 2014, Poekes, Lanthier, and Leclercq 2015).

1.4 Introduction to the study

Given the fact that overweight and obesity are on the rise worldwide, weight reduction and weight regulation is a highly relevant topic. In order to maintain a healthy weight, Norwegian Health Authorities recommend a diet consisting of 45-60 % of energy (E%) from carbohydrates, 25-40 E% from fat and 10-20 E% from protein (Helsedirektoratet 2014). Whether this is the most optimal distribution of macronutrients, is now under debate. In recent years, diets with a higher proportion of protein and/or fat, has gained increased interest as methods of weight reduction and weight management. However, studies have shown that HP diets differ in obesogenic potential, depending on the protein source used. Tastesen et al. found that mice fed casein and cod/scallop remains lean, whereas mice receiving chicken develop obesity (Tastesen, Ronnevik, et al. 2014). In another study carried out by our research group, mice were fed HP diets with either casein, soy, cod, beef, chicken or pork as protein source (Liisberg, Myrmel, et al. 2016). This study showed that casein stands out as the most efficient protein source in preventing weight gain. Mice fed cod and beef protein had an increased body weight gain compared to the mice fed casein, but to a lesser extent than mice fed pork or chicken. The diets based on chicken and pork were highly obesogenic, even more so than a high fat/high sucrose control diet. Furthermore, mice fed the HP casein diet maintained a classic morphology in their interscapular BAT (iBAT), whereas brown adipocytes in mice fed pork and chicken had a morphology much more like white adipocytes, with fewer and larger lipid droplets.

Of notice, these protein sources varies in endogenous fat composition. Cod contains higher levels of n-3 FAs compared to chicken and pork, which are higher in the n-6 FAs. It is known that n-3 FAs, especially when they originate from phospholipids, can have an anti-obesity effect (Alvheim et al. 2012, Rossmeisl et al. 2012, Liisberg, Fauske, et al. 2016). Therefore, the differences in obesogenic potential of these HP diets may be a consequence of a different amino acid composition, a different fatty acid composition or a combination of the two.

1.5 Aims of the study

In this study, pangasius (Pangasianodon hypophthalmus), an Asian shark catfish, was introduced as a new protein source. The amino acid composition of pangasius is similar to cod (table A.2, appendix I) and the fatty acid composition is similar to chicken (table A.4, appendix I). Feeding one group pangasius, as well as having a chicken- and a cod-fed group, could therefore give the opportunity to distinguish between the effect of the amino acid- and the fatty acid composition. Furthermore, one group received a restricted amount of the chicken-diet. The goal of this restriction was to keep the mice lean and investigate whether the change in iBAT morphology in mice fed chicken is caused by the protein source itself, or rather a consequence of obesity. Given that changes in iBAT morphology may affect thermogenesis and energy expenditure, we also wanted to assess expression of genes involved in metabolic processes in this tissue.

To summarize, the aims of this study were as following:

- To investigate whether differences in the amounts of n-3 and n-6 FAs may contribute to the varied obesogenic potential of different HP diets
- To evaluate the effect of different protein sources on glucose homeostasis
- To study if the "whitening" effect of chicken as a protein source on iBAT morphology is caused by the protein source itself, or rather a consequence of obesity
- To review the impact of different protein sources on gene expression and UCP1 levels in iBAT

2.0 Materials and methods

2.1 The animal experiment

The mice used in this experiment were C57BL/6J BomTac mice (figure 2.1). This mouse model was chosen due to its ability to develop obesity, hyperglycemia and hyperinsulinemia when fed a HF diet (Black et al. 1998, Surwit et al. 1988). Eighty male mice were bought from Taconic Europe (Ejby, Denmark) at a weight of approximately 25 g. Upon arrival, the mice had a seven-day acclimatization period, during which a body scan was performed. Seventy of the mice was then divided into seven groups (n=10) based on body weight, lean mass and fat mass. Each group received a different diet. Two of the groups were reference groups, receiving either a LF or a high fat/high sugar (HF/HS) diet. The remaining five groups received high fat/high protein (HF/HP) diets containing four different protein sources: Casein, cod, pangasius or chicken. The reference groups and four of the HF/HP groups were fed *ad libitum*, whereas the last group was given a restricted amount of the HF/HP chicken-based diet. Feeding was carried out three times a week for 12 weeks prior to termination.

Figure 2.1 Private photo of a C57BL/6J BomTac mouse from the experiment

2.1.1 Ethical statement

This animal experiment were approved by the Norwegian Animal Health Authorities (ID nuber FOTS: 5358). No harmful effects were observed during the trial.

2.1.2 Diets

The four experimental HF/HP-diets, containing ~ 41 g protein and ~24,5 g fat /100 g, were produced at NIFES. Reference diets were a pre-bought LF diet (Ssniff Spezialdiäten GmbH, Germany) and a HF/HS diet (Ssniff Spezialdiäten GmbH, Germany).

Figure 2.2 Grouping

One group received casein as their protein source, one cod, one pangasius and two groups received chicken (figure 2.2). The first six groups were fed *ad libitum*, whereas the last group was given a restricted amount of the chicken-based diet. The objective of this restriction was to keep the mice at the same weight as the mice in the casein-fed group. After two weeks of experimental feeding, the amount of feed given to the restricted chicken group was reduced by 38 % compared to the other groups. The amount of feed given was further reduced later on (table 2.1), as the mice in this group gained more weight than the individuals in the casein-group despite feed restriction.

Table 2.1 Amount of feed given to the restricted chicken- fed group.

Week	Feed given (g/day)	Restriction* (%)
2	2	38
3	1,8	44
6	1,65	49
9	1,6	51

*all other HF/HP-groups recieved 3,25 g feed/day

2.1.3 Preparation of the diets

The chicken (Solvinge renskåret kyllingfilet, Rema 1000), cod (Fiskemannen, Rema 1000) and pangasius (Godehav skinn- og benfri filet, Polar Seafood Denmark, Rema 1000) were warm-treated, freeze-dried and homogenized at NIFES. All ingredients were weighted on a Mettler Toledo PG42002-S/PH weight, mixed in a Crypto Peerless EF20 blender and then stored at -20 ^{0}C. Diet composition are displayed in table A.1 in appendix I along with AA- and FA- composition of the diets (table A.3 and A.5 respectively).

2.1.4 Housing and feeding

The mice were single caged (Tecniplast 1291) and kept in a termoneutral room (28-30 ^{0}C). The room had a 12-hour light/dark cycle. Each cage was equipped with wooden bedding, nesting material, a house and a chewing stick. Feeding was carried out three times a week; Monday, Wednesday and Friday. Total feed intake was measured during the entire experiment by weighing the feed before feeding as well as weighing the remains that were left when the mouse was given a new meal. When changing cages, the bedding in the old cages was shifted and feed residue was collected and weighted. Changing of cages took place every second week. The water bottles were changed once a week.

2.1.5 Measurements

Once a week, all the mice were weighted on a Mettler Toledo (PG42002-S/PH) weight. A body scan was performed at baseline and after nine weeks. The scan was conducted using a Bruker Minispec LF50mq 7.5 magnetic resonance imaging (MRI) apparatus. This apparatus uses a magnetic field to distinguish between fat mass, lean mass and free water, thus giving information on the animal's body-composition.
In week nine, the wooden bedding in the cages was replaced with a paper cover. In the end of the week, all feces were collected. The feces was analyzed for fat and nitrogen content and this was further used to calculate apparent nitrogen- and fat digestibility. Technicians at NIFES analyzed fat and nitrogen content as described in (Tastesen, Ronnevik, et al. 2014). Apparent digestibility was calculated using the following formula:

$$\text{Apparent digestibility} = \frac{\text{amount of fat/nitrogen eaten} - \text{amount of fat/nitrogen excreted}}{\text{amount of fat/nitrogen eaten}} \times 100\ \%$$

2.1.6 Insulin tolerance test

An insulin tolerance test (ITT) was conducted after ten weeks of experimental feeding. Prior to testing, the mice were transferred to a clean cage containing wooden bedding and their house. The mice were in a randomly fed state. Each mouse was injected intraperitoneally with insulin (1.00 U/kg lean mass). A small slit was made to puncture the tail vein, and blood glucose was measured with a glucometer (Contour, Bayer) at baseline and 15, 30, 45 and 60 minutes after injection. After testing, all tails were sterilized with 70% ethanol (EtOH) in order to prevent infection.

2.1.7 Oral glucose tolerance test

After eleven weeks, an oral glucose tolerance test (OGTT) was performed. Five hours before testing, the mice were weighted and moved to clean cages equipped with wooden bedding and their house. After a five hour fasting period and a new weighting, a small incision to puncture the lateral tail vein was made. Blood glucose was measured with a glucometer (Contour, Bayer) and 20 µl blood was collected in an EDTA coated minivette and transferred to an eppendorf tube. An oral dose of glucose (3 mg/g lean mass) was given. Blood glucose was measured 15, 30, 60 and 120 minutes after glucose administration. 20 µl blood was also collected after 15 and 30 minutes. All collected blood was centrifuged at 1000 x g for 5 minutes at 4°C, 7 µl plasma was collected and subsequently stored at - 80°C for further testing (described in Section 2.3) When testing was finished, all tails were sterilized with 70% EtOH.

2.1.8 Termination

Upon termination, all mice were weighted. Termination was executed in a randomly fed state. The mice were anesthetized with isofluran (Isoba-vet, Schering Plough, Denmark) by putting them in a Univentor 400 Anesthesia Unit Apparatus (Univentor Limited, Sweden). Euthanasia

was performed by cardiac puncture. Blood from the heart was collected with a syringe connected to a tube containing an EDTA anticoagulant. The samples were then centrifuged at 2500 x g at 4°C for five minutes. Plasma and red blood cells were stored separately at -80 °C for further analysis.

Four different adipose tissues were dissected at the termination point: Retroperitoneal white adipose tissue (rWAT), epididymal white adipose tissue (eWAT), inguinal white adipose tissue (iWAT) and interscapular brown adipose tissue (iBAT), the first two being visceral adipose tissues whereas the two latter is subcutaneous. Additionally, the liver, kidneys and intestine were excised, as well as one muscle: *m. Tibialis anterior*. Samples for histology were collected and fixated in 4 % formaldehyde. Tissues for qPCR or other testing were snap frozen in liquid nitrogen and stored at -80 °C. Duodenum, jejunum, ileum and colon were also collected and stored in eppendorf tubes at -80 °C for further analysis.

2.2 Histology

2.2.1 Fixation

Samples from liver, iBAT, eWAT and iWAT were placed in a plastic cassette at termination and fixated in 4% formaldehyde in 0,1 M phosphate buffer (PB) overnight. The samples were then transferred to 0,1 M PB and stored at 4 ^{0}C upon the following dehydration.

2.2.2 Dehydration and paraffin infiltration

To remove fixation solutes and water from the tissue sections, the PB was replaced with gradually increasing concentration of alcohol (Table A.6, appendix II). When the tissues were completely dehydrated in 100 % alcohol, the alcohol was replaced with xylene. This is a medium soluble in both alcohol and paraffin. Paraffin (Histolab, Sweden) was then heated to 59 °C in a transportable heater and the samples were placed in the paraffin overnight to remove the xylene.

2.2.3 Embedding in paraffin

Prior to embedding, the paraffin was replaced once to remove traces of xylene (Table A.6, appendix II). The samples were then embedded using a EC 350 Paraffin embedding center (Microtom International GmbH, Germany). A small amount of paraffin was applied to the

bottom of a metal mold. After removing the top of the plastic cassette, the tissue samples were placed in the mold and fastened by leaving it on the cold component for a short while. The bed of the cassette was placed over the mold, and this was filled with paraffin and left on the cold board until completely stiffen. The block of paraffin was then removed from the mold.

2.2.4 Sectioning and staining

Prior to staining, the samples were sectioned at Molecular Imaging Center at Haukeland University Hospital. The slides were 5µm thick. A rehydration was then performed, followed by a staining with hematoxylin and eosin (H&E). The procedure was executed in a ventilation chamber. Time schedule and solutions are listed in table A.7, appendix II. Hematoxylin stains the nucleus of the cells, whereas eosin adds color to the cytoplasm. After staining, the slides were mounted with a xylene based glue (Entellan, Sigma) and left to dry in the ventilation chamber overnight.

2.2.5 Immunohistochemistry

Immunohistochemistry was performed in order to investigate the presence of UCP1 in iBAT, and differences between the experimental groups.

Upon the immunohistochemistry process, rehydration was necessary to make the tissues more reactive (table A.8, appendix III). The different steps of the immunohistochemistry are listed in table A.9 in appendix III along with content of the different reagents and solutions. Citrate buffer was heated in a water bath, and was used in order to make the epitopes more available. Between each treatment, phosphate-buffer saline (PBS) was used to wash the slides. To avoid oxidation by peroxidases, H_2O_2 in methanol (MetOH) was applied. Incubation with goat serum was necessary in order to avoid background staining. The primary antibody binds to the epitope on the UCP1-protein, whereas the secondary antibody binds to the primary. Avidin-biotin-peroxidase-complex (ABC) binds to the secondary antibody. Further, diaminobenzidin tetrahydrochloride (DAB) was applied. ABC oxidizes DAB, causing precipitation and a coloring of the antigen-antibody-complex. Finally, the nuclei were colored with hematoxylin and dehydration (table A.8, appendix II) was performed. The slides were mounted with a water-soluble glue (ImmunoHistoMount, Sigma) and left to dry overnight.

2.2.6 Microscopy

Inspection of cell morphology of iBAT and iWAT, as well as UCP1 expression of iBAT, was carried out using an Olympus BX 51 binocular microscope. A representative field from each tissue section was photographed with an Olympus DP50 3.0 camera. Adipozyte size was determined by Adiposoft (Galarraga et al. 2012). UCP1 expression was quantified by ImageJ.

2.3 Ultra Sensitive Mouse ELISA Insulin Kit

The Ultra Sensitive Mouse Insulin ELISA Kit (Crystal Chem Inc., USA) is a kit for the quantitative determination of insulin in mouse serum, plasma and fluid. This kit was used to measure insulin levels in plasma collected at the start of the OGTT-test and 15 minutes after glucose distribution. Reagents are listed in table A.10 in appendix IV. Method was performed according to the protocol given by the manufacturer.

Prior to assay procedure, a preparation of working mouse insulin standards was necessary. 150 µl of sample diluent and 50 µl of mouse insulin stock solution (25,6 ng/ml) was mixed in a microtube, giving the mix an insulin concentration of 6,4 ng/ml. Sample diluent was also added to seven more tubes, 50 µl in each. 50 µl of the 6,4 ng/ml standard was then added to the first tube containing only sample diluent. This was mixed thoroughly and 50 µl was then added to the second tube and so on (figure 2.3)

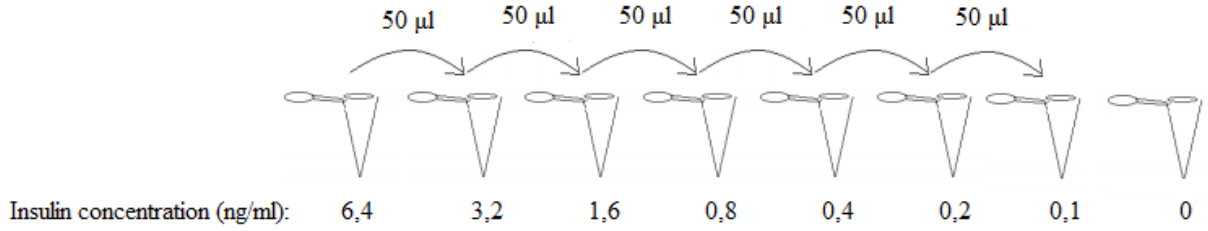

Figure 2.3 Preparation of working mouse insulin standards

In a microplate containing 96 anti-insulin antibody-coated wells, 95 µl of sample diluent was added to each well. 5 µl of each sample and the insulin standards was then distributed on the plate, which was further incubated for 2 hours at 4^0C. This allowed for insulin in the samples to bind to the guinea pig anti-insulin antibody coated on the microplate wells. Following incubation, unbound material was removed by washing the wells with wash buffer. The

washing was performed using an automatic plate washer (1296-026 Delfia Platewash). A second reaction was then carried out by adding 100 µl of anti insulin enzyme conjugate in each well. The plate was then incubated at room temperature for 30 minutes, followed by a new washing. In this second reaction, horse radish peroxidase (POD)-conjugated insulin antibody is bound to the guinea pig anti-insulin antibody/mouse insulin complex. Immediately after the second washing, 100 µl of enzyme substrate solution (TMB) was dispersed in each well and reacted for 40 minutes in room temperature. In this third reaction, the bound POD-conjugate reacts with the clear TMB-solution, converting it to a colored product. The reaction was stopped by adding 100 µl per well of enzyme stop solution. Conclusively, absorbance at 450 and 660 nm was measured with a spectrophotometric plate reader (VictorX5, Perkin Elmer) and the results were calculated.

2.4 Reverse Transcription qPCR

A reverse transcription (RT) quantitative real-time polymerase chain reaction (qPCR) was carried out to identify relative gene expression of several brown markers in iBAT. Upon the qPCR, RNA-purification and -precipitation were necessary, as well as measuring RNA integrity and doing a reverse transcription from RNA to cDNA.

2.4.1 Homogenization and RNA-purification

Agencourt RNAdvance Tissue Kit (Beckman Coulter, USA) was used to retrieve purified RNA from iBAT. Reagents and prepared solutions are listed in table A.11 in appendix V. First, tissue samples were homogenized. The samples were transferred to tubes containing 2 zinconium beads and 630 µl lysis buffer and homogenized using a Precellys 24 lysis & homogenization instrument (Bertin Technologies, France) at 5500 rpm for 2 x 30 seconds. The tubes were then spun down and incubated at 37 ^{0}C for 25 minutes. Further, two 12 000 x g centrifugations at 4^{0}C were carried out. Following the first and second centrifugation, the aqueous phase were transferred to a new tube. 400 µl binding buffer was then added to the lysate and a 5 minute incubation followed. The tubes were further incubated for 6 minutes on a magnetic rack, the supernatant was removed and the tubes were removed from the magnetic rack. 800 µl wash buffer was added and a 5 minutes incubation on the magnetic rack followed. Further, supernatant was removed, the tubes were removed from the magnetic rack and 800 µl 70% ethanol was added. A new 5 minutes incubation on the magnetic rack was

carried out, followed by removal of the supernatant and two more ethanol-washes on magnet with a 2 minutes incubation in between. After the last ethanol-wash was carried out, the tubes were removed from the magnetic rack and left to dry for 10 minutes. Finally, 40 µl MQ-water was added and samples were incubated for 2 minutes before being moved to the magnetic rack and given a final 8-minute incubation. The eluate was transferred to a new tube and RNA concentration was measured with Nanodrop ND-1000 spectrophotometer (Saveen Werner, Sweden). The measurement with the Nanodrop also gives information regarding sample quality by measuring absorbance and calculating the A260/A280- and A260/A230-ratios.

2.4.2 RNA-precipitation

As measurements made with the Nanodrop spectrophotometer revealed unsatisfying 260/230-ratios, RNA-precipitation was necessary. 100 µl ice-cold ethanol and 4 µl 3M NaAc (pH 5,2) was added to each sample, and they were further stored at -80 °C overnight. Precipitation was carried out by spinning the samples in a centrifuge at 12 000 x g at 4 °C for 20 minutes. Supernatant was removed and 1 ml ice-cold 75% EtOH was added. After a 5 minutes centrifugation, supernatant was removed once more and 15 µl water was added. The Nanodrop ND-1000 was used to measure concentration and ratios.

2.4.3 Measuring RNA integrity, Bioanalyzer

RNA integrity was measured using Agilent 2100 Bioanalyzer (Agilent Thechnologies, USA) and an RNA 6000 Nano LabChip kit (Agilent Technologies, Germany). Each RNA chip contains an interconnected set of microchannels. In the BioAnalyzer, nucleic acid fragments are driven through the channels by electrophoresis and separated based on their different sizes.

Upon procedure, RNA dye concentrate was equilibrated to room temperature. The concentrate was then vortexed and spun down before 0,5 µl was added to a tube containing 32,5 µl RNA gel matrix. Further, centrifugation (10 min, 13 000 x g, room temperature) was needed before placing the chip in the priming station and pipetting 9 µl gel-dye mix in the well marked G. The plunger was positioned at 1 ml and the chip priming station was closed. After 30 seconds, the plunger was released. 9 µl of gel-dye mix was added to two more wells, and 5 µl of RNA marker were added to all wells. Furthermore, 1 µl of ladder were added to a marked well and

1 µl of the samples distributed in the twelve sample-wells. Twelve randomly selected samples were used. Finally, the chip was placed in the Agilent 2100 Bioanalyzer. Two chips, containing in total 24 samples, were measured.

2.4.4 Reverse transcription reaction

To convert the single stranded RNA to double stranded cDNA, a RT reaction was performed. All samples were individually diluted to a concentration of 50 ≤ ± 3% ng/µl. The Nanodrop spectrophotometer was used to measure concentrations. Further, to make a standard curve, 2 µl from 35 of the samples were pooled in a new tube. Concentration was measured and a 100 µl solution with the concentration of 100 ng/µl was prepared. A double dilution was carried out, resulting in six solutions with decreasing concentrations (Figure 2.4).

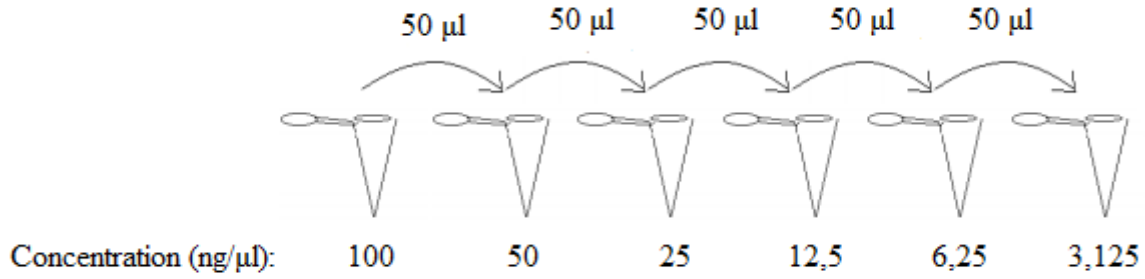

Figure 2.4 Preparation of solutions for standard curve

A RT-reaction mix was prepared (table A.12, appendix V). Two negative controls were included, a non- amplification control (without multiscribe enzyme, NAC) and a non-template control (without RNA, NTC). To a 96-well RT-plate 40 µl RT-reaction mix was added to all wells (except the NAC-well). Further, 10 µl of each RNA-sample was distributed on the plate. Water was added to the NTC-well. A clean plate cover was put on and the plate was centrifuged (50 G, 1 min, room temperature). Conclusively, a Gene AMP PCR System 9700 PCR machine (Applied biosystems) was used for the RT-reaction. The program is presented in appendix V, table A.13. Upon qPCR, the plate was stored at -20 ºC.

2.4.5 Quantitative real time polymerase chain reaction

To quantify gene expression in iBAT, qPCR was conducted. Volume of the cDNA plate was doubled by adding 50 µl ddH_2O in each well. Further, the cDNA plate was centrifuged (1000 x g, 1 minute) and vortexed (1300 rpm, 5 minutes). Real time PCR mix was made according to table 2.2 and distributed to an eight-well strip (112 µl/well). Primer names and sequences are presented in table A.14, appendix V. Pipetting was carried out by robot (Biomek® NX^P Laboratory Automation Workstation, Beckman Coulter USA), adding 2 µl of sample cDNA and 8 µl PCR mix to a 384-wells Real Time plate. The plate was further covered with an adhesive optical cover and centrifuged for 2 minutes at 1500 x g. qPCR was performed using a Light Cycler 480 instrument (Roche Diagnostics). Due to group variations in housekeeping genes measured, cp-value was used to calculate amounts of mRNA and relative gene expression.

Table 2.2 Real time PCR mix

Reagent	Volume (µl)
ddH_2O	330,6
Primer (forward)	5,7
Primer (reverse)	5,7
SYBR Green PCR Master Mix	570

2.5 Statistical analysis

Processing of raw data was carried out in Microsoft Excel 2013. GraphPad Prism 6 was used to identify outliers by Grubb's test. Normality was determined by D'Agostino-Pearsons test and equality of group variances stated by Brown-Forsythes test. GraphPad was also used to perform a one-way analysis of variance (ANOVA) with Fisher's LSD multiple comparisons post hoc test. Growth, feed intake as well as data from ITT and OGTT were analyzed by repeated-measurements (RM) ANOVA with Fisher's LSD. Finally, as the normality assumption of a one-way ANOVA was not met, Kruskal-Wallis test was performed on data on apparent fat absorption. The reference groups were excluded from the statistical analysis, but are shown as scattered lines. All data are presented as mean ± SEM. Group means were considered statistically different at $p \leq 0.05$ and differences are marked by different letters.

3.0 Results

The different experimental diets varied in obesogenic effect and lead to differences in body weight development as well as in body composition. Observations made throughout the animal experiment, including body weight development, energy intake and changes in insulin sensitivity and glucose tolerance will be presented in the first three sections. The last sections focuses on observations made post termination, such as changes in adipocyte size and morphology as well as differences in gene expression. Body weight gain and energy intake are presented up to week nine of the experiment due to the possible impact of ITT and OGTT, conducted in week ten and eleven respectively, on feeding behavior. In order to differentiate the calorie restricted chicken-fed group from the one fed *ad libitum*, this group are referred to as the "chicken (restricted)-group".

3.1 Body weight development and body composition

3.1.1 Body weight development

Different HP diets had a different effect on body weight development, as presented in figure 3.1. A HF/HP diet based on chicken, pangasius and cod were obesogenic relative to a casein-based diet. After nine weeks the pangasius-fed mice had a greater body weight gain than the group fed cod. Furthermore, there was a trend towards higher weight gain in the group fed chicken compared to the pangasius fed-group ($p = 0.095$). Analysis with RM ANOVA (figure 3.1 A) underlines this. The mice fed casein had the lowest weight gain, although not significantly different from the chicken (restricted)-fed group (figure 3.1 B).

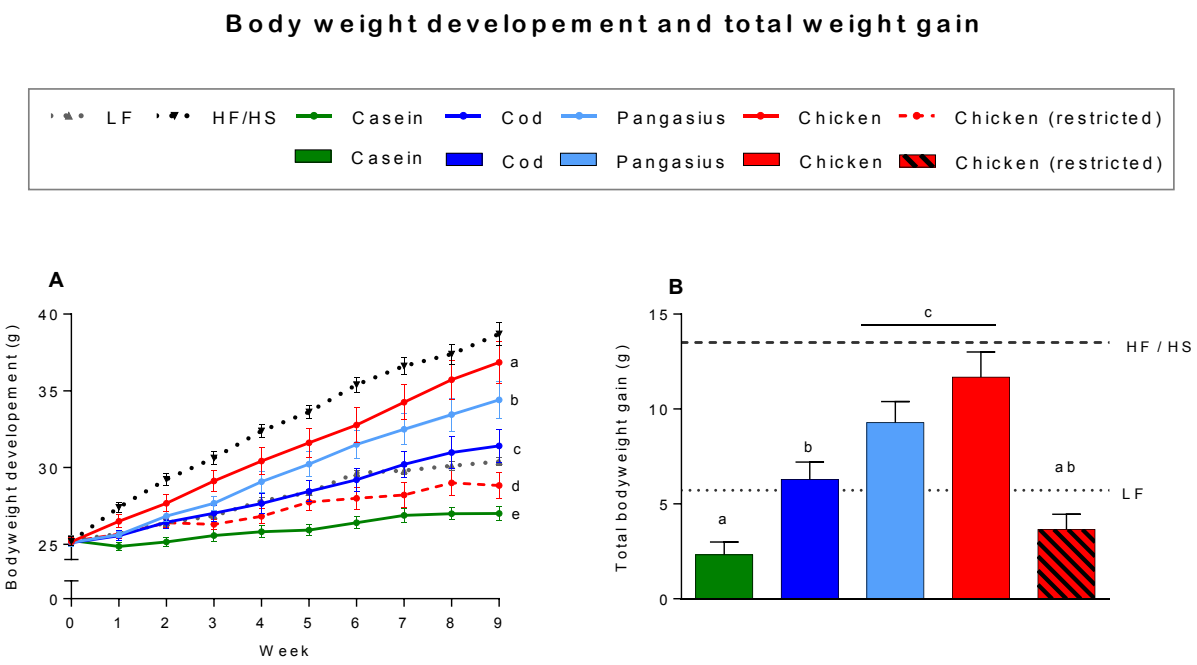

Figure 3.1 Body weight development and total weight gain. Body weight development (A) and total weight gain (B) after nine weeks. Body weight development was analyzed by RM ANOVA. Total body weight gain was analyzed using a one-way ANOVA with multiple comparison (uncorrected Fisher's LSD) of the mean of each experimental group. Results are presented as mean ± SEM. Statistical differences ($p \leq 0.05$) are marked by different letters.

3.1.2 Body composition

To further investigate if weigh gain was due to an increased amount of fat mass or lean mass, an MRI-scan was performed at the beginning of the experiment and after nine weeks. Results from MRI-scan at week nine are displayed in figure 3.2. The higher weight gain observed in the chicken-fed group is mainly due to increase in fat mass (figure 3.2 A, D). Furthermore, when pangasius was used as protein source, the mice gained more fat than those fed cod, but less than those fed chicken (figure 3.2 B). In contrast to other groups, mice in the group fed casein had a slight decrease in fat mass. In this group, weight gain was mainly due to increased lean mass (figure 3.2 D). Interestingly, when chicken was used as protein source instead of cod or casein, the mice gained less lean mass (figure 3.2 D). This did not seem to be a consequence of weight gain, as similar results was observed in the chicken (restricted)-group. Pangasius as protein source had an intermediate effect (figure 3.2 C-D).

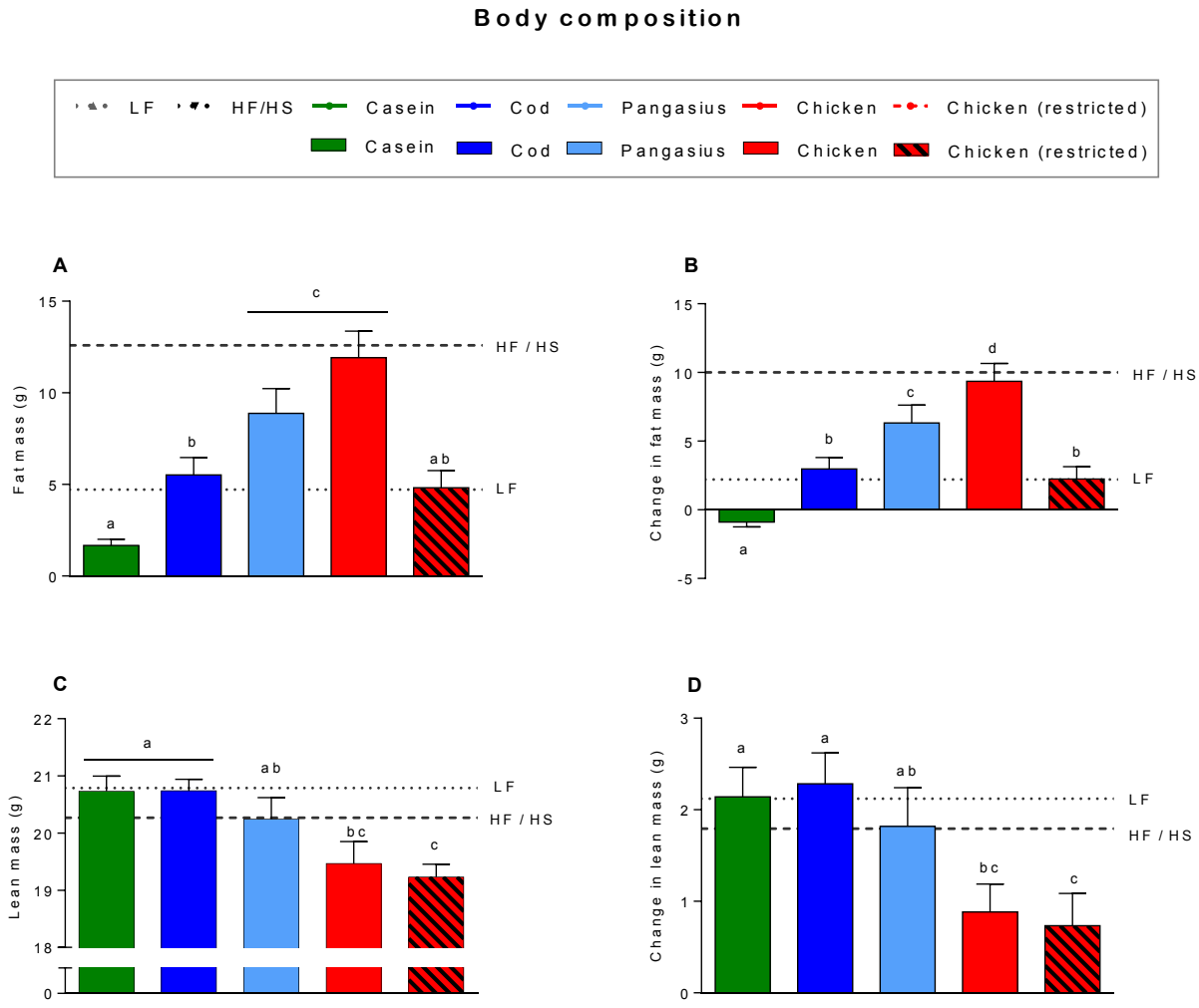

Figure 3.2 Body composition. MRI-scan was used to detect changes in body composition. Total fat mass (A), change in fat mass relative to baseline (B), total lean mass (C) and change in lean mass relative to baseline (D). Group variations were analyzed using a one-way ANOVA with multiple comparison (uncorrected Fisher's LSD) of the mean of each experimental group. Results are presented as mean ± SEM. Statistical differences ($p \leq 0.05$) are marked by different letters.

3.2 Energy intake, feed efficiency and digestibility

Throughout the entire experiment, feed given as well as remains were weighted to monitor each mouse's total feed intake. This was used to calculate total energy intake and investigate if the differences in weight gain were caused by differences in energy intake.

Figure 3.3 B reveals that mice fed casein, the group with the lowest body weight, had the highest energy intake as well as the chicken-fed mice. Further, mice fed chicken ate more than mice fed cod. The group fed pangasius had an intermediate energy intake compared to these two. RM-ANOVA analysis is in the affirmative (figure 3.3 A).

Based on energy intake, weight- and fat mass gain, feed efficiency was calculated (figure 3.3 C-D). Chicken as protein source had significantly higher feed efficiency compared to casein or cod. The casein-based diet had lower feed efficiency than all other groups, whereas the pangasius-based diet had an intermediate effect compared to the cod- and chicken-based diets. When measured in fat gain, feed efficiency of pangasius was significantly elevated compared to cod (figure 3.3 D). Furthermore, feed efficiency of the chicken-based diet declined in the chicken (restricted)-group (figure 3.3 C).

Differences in weight gain may be caused by variations in digestibility of macronutrients in the diet. In order to investigate this, fat and nitrogen content of feces was analyzed and apparent fat- and nitrogen-absorption was calculated (figure 3.3 E-F). Mice fed casein had a significant lower nitrogen digestibility than mice fed pangasius, but not compared to any other group (figure 3.3 E). The group fed cod had lower fat digestibility than mice fed casein and chicken, whereas pangasius as protein source had an intermediate effect (figure 3.3 F). Comparing the two chicken-fed groups, no significant differences in fat- or nitrogen absorption were observed.

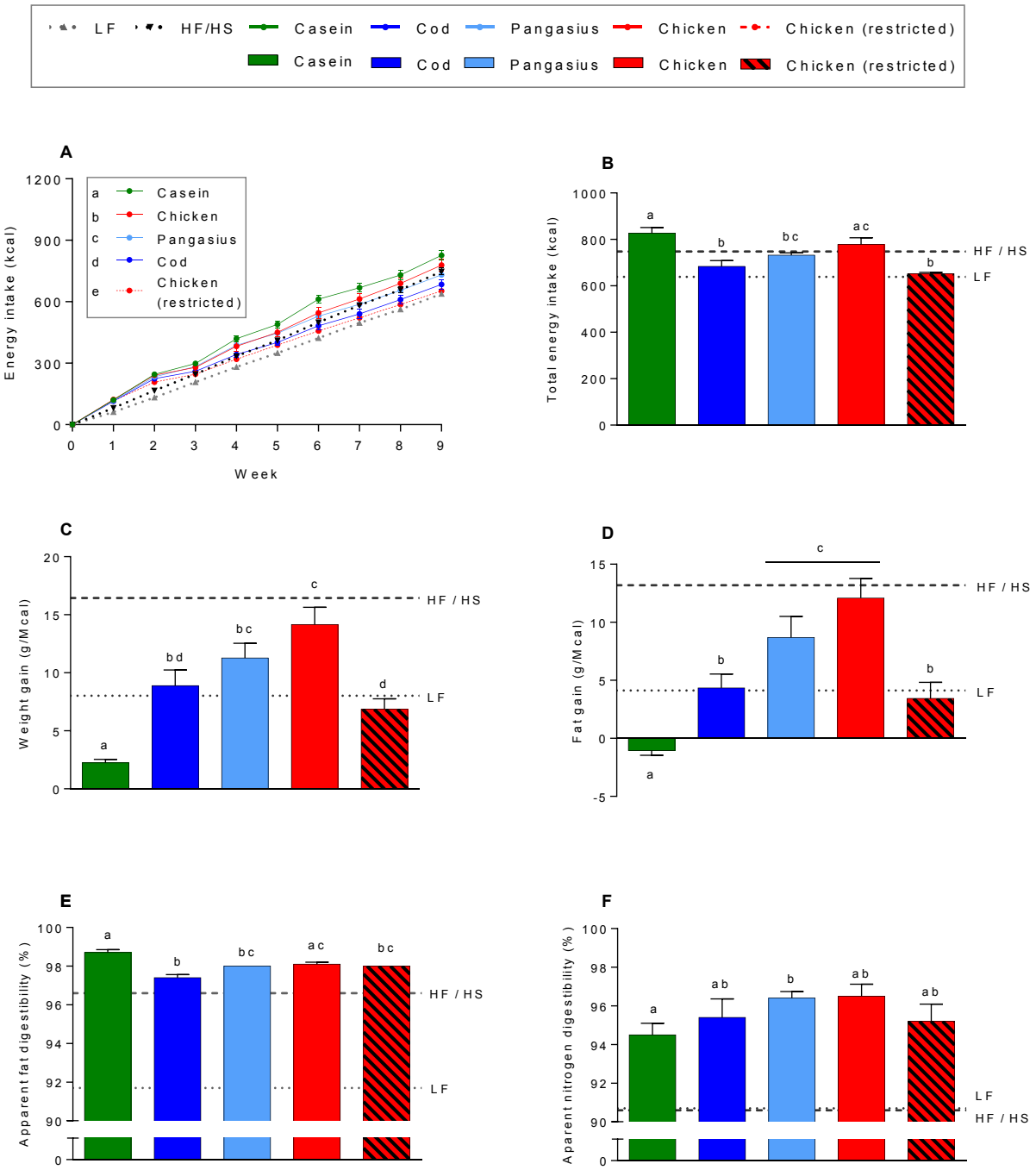

Figure 3.3 Energy intake, feed efficiency and apparent fat and nitrogen digestibility. Energy intake from baseline to week nine (A), accumulated energy intake (B), feed efficiency measured in total weight gain (C), feed efficiency measured in total fat gain (D), apparent fat digestibility (E) and apparent nitrogen digestibility (F). Development in energy intake was analyzed by RM ANOVA. Feed efficiency and nitrogen digestibility were analyzed using a one-way ANOVA with multiple comparison (uncorrected Fisher's LSD) of the mean of each experimental group. Fat digestibility was analyzed by Kruskal-Wallis test. Results are presented as mean ± SEM. Statistical differences ($p \leq 0.05$) are marked by different letters.

3.3 Insulin sensitivity and glucose tolerance

3.3.1 Insulin tolerance test

After ten weeks, an ITT was performed in order to assess the impact of different protein sources on insulin sensitivity. Results are presented in figure 3.4. Analysis by RM ANOVA demonstrates that mice fed chicken and pangasius had impaired insulin sensitivity compered to all other groups (figure 3.4 A). Although no significant differences, calculated area over the curve (AOC) seems to substantiate this (figure 3.4 C). AOC appeared to decline when body weight inclined. Fifteen minutes post insulin injection, blood glucose levels had declined significantly more in mice fed casein compared to those fed chicken and pangasius, suggesting higher insulin sensitivity in this group (figure 3.4 D). Insulin response after fifteen minutes mirrored body weight. After thirty minutes, change in blood glucose was only significantly different between the group fed casein and the one fed pangasius (figure 3.4 E). Few significant differences were observed in fasting blood glucose, but the mice fed chicken (restricted) had lower blood glucose levels than mice fed cod, pangasius and chicken (figure 3.4 B).

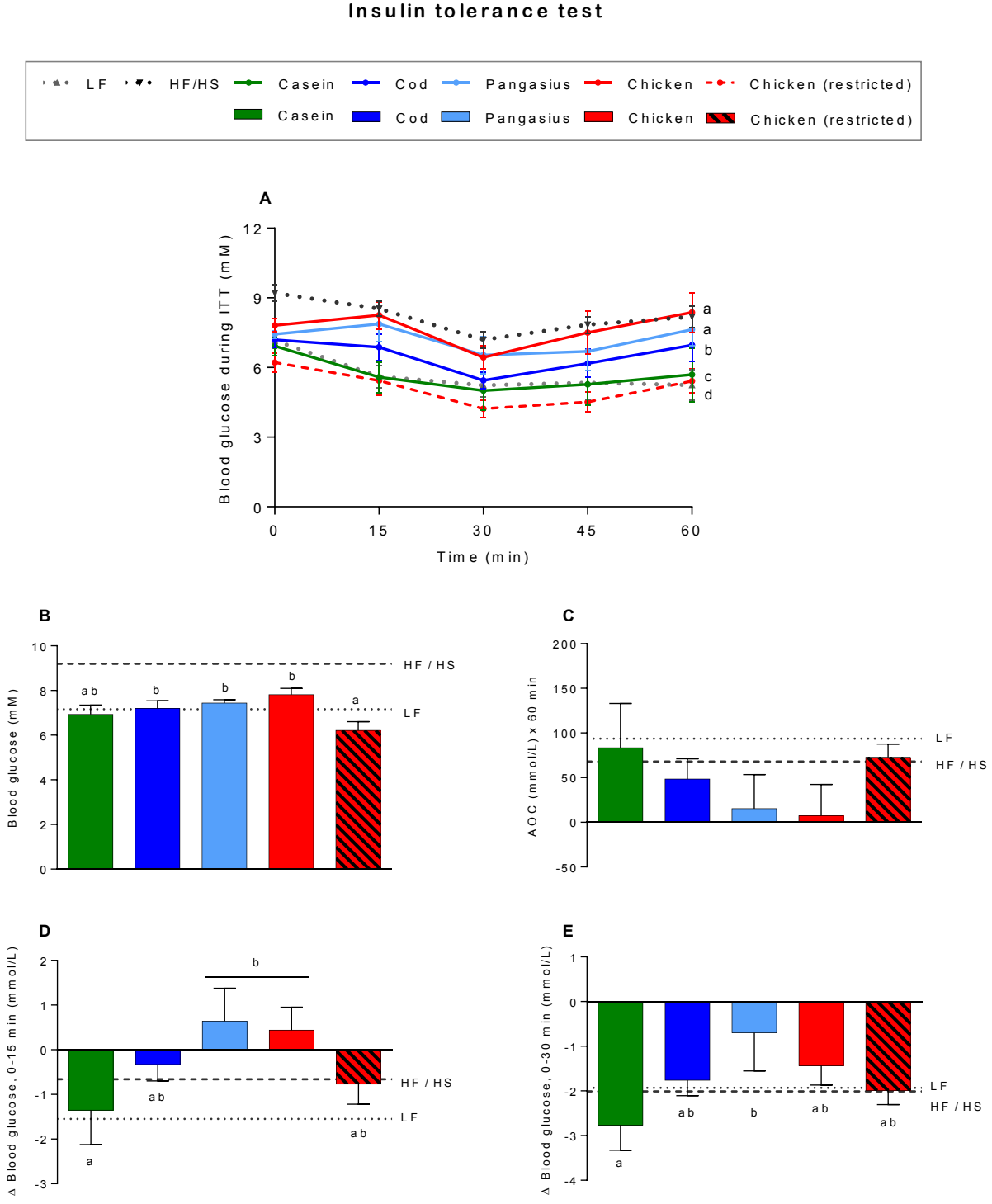

Figure 3.4 Insulin tolerance test. Blood glucose measured during ITT (A), fed blood glucose (B), area over the curve (AOC) (C), delta blood glucose 15-0 minutes (D) and delta blood glucose 30-0 minutes (E). Blood glucose levels during ITT were analyzed by RM ANOVA. Data B-E were analyzed by one-way ANOVA with multiple comparison (uncorrected Fisher's LSD) of the mean of each experimental group. Results are presented as mean ± SEM. Statistical differences ($p \leq 0.05$) are marked by different letters.

3.3.2 Oral glucose tolerance test

To evaluate the impact of the different diets on glucose tolerance, an OGTT was performed after eleven weeks. The results are presented in figure 3.5. Upon glucose administration, mice fed chicken (restricted) had significantly lower blood glucose levels compared to those fed *ad libitum* (figure 3.5 B). RM ANOVA analysis of blood glucose data during the test shows that mice fed chicken had reduced glucose tolerance compared to mice fed cod (figure 3.5 A). Pangasius-fed mice was neither different from those fed chicken, nor those fed cod. Mice fed chicken (restricted) had better glucose tolerance than those fed *ad libitum*, suggesting that reduced glucose tolerance was associated with high body weight. However, calculated incremental area under the curve (AUC) (figure 3.5 C), which calculates response to glucose administration independent of blood glucose levels at baseline, reveals that the two chicken-fed groups had a similar response, together with the groups fed casein and cod.

Ultra Sensitive Mouse Insulin ELISA kit was used to measure insulin concentrations in plasma collected upon testing and 15 minutes post glucose administration (figure 3.5 D-E). Figure 3.5 D demonstrates elevated fasting plasma insulin levels in mice fed pangasius and chicken compared to mice fed casein or chicken (restricted). Moreover, fasting plasma insulin levels in the group fed pangasius was significantly higher compared to the group fed cod. Plasma insulin levels measured after 15 minutes indicates that mice fed chicken had reduced insulin sensitivity compared to mice fed casein, cod and pangasius (figure 3.5 E). However, this only seemed to be the case when the mice were fed chicken *ad libitum* and consequently was obese. High levels of fasting plasma insulin in mice fed pangasius indicates impaired insulin sensitivity. Moreover, compared to the chicken-fed mice, this group did not compensate by secreting higher amounts of insulin post glucose administration (figure 3.5 E), which caused a high AUC.

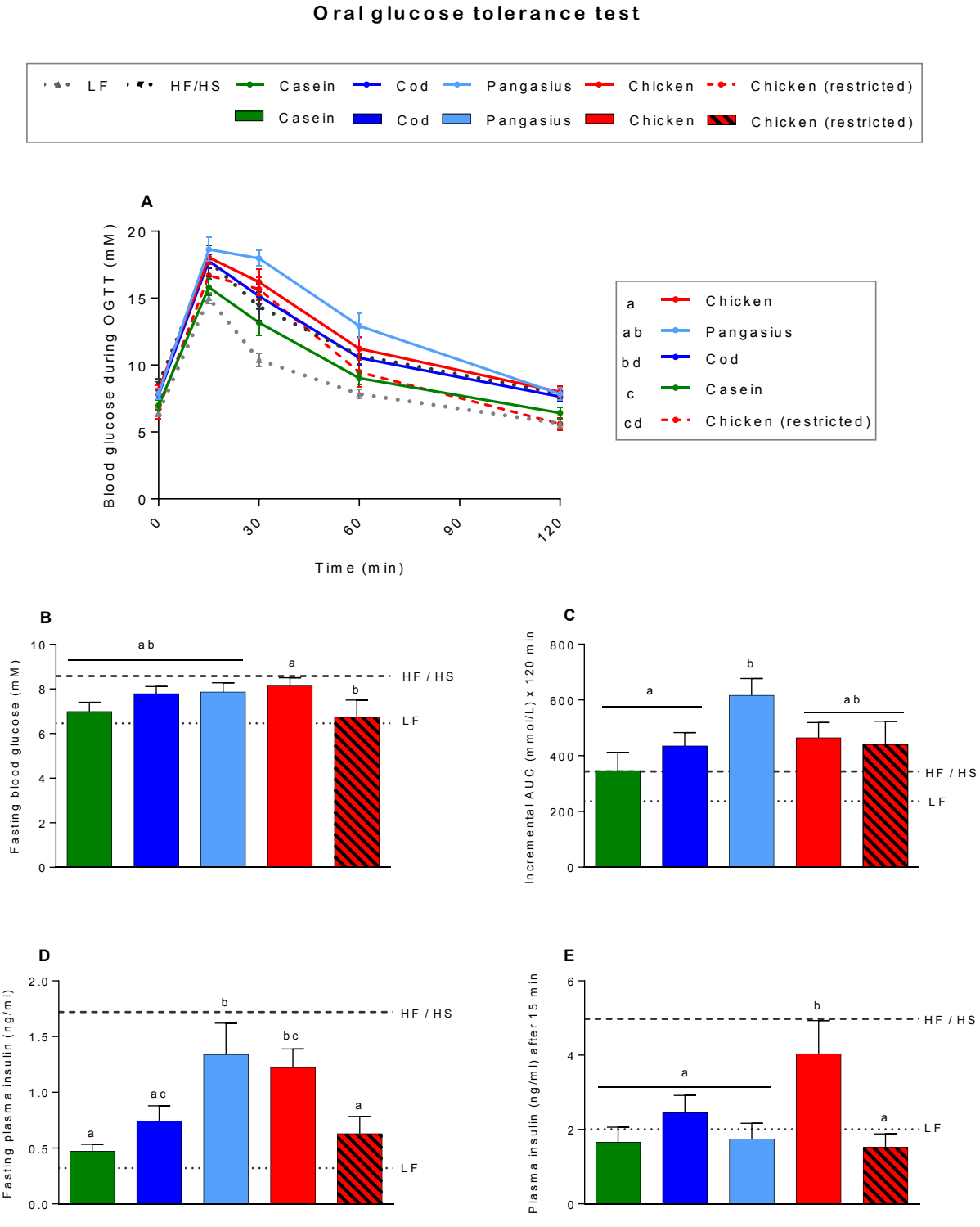

Figure 3.5 Oral glucose tolerance test. Blood glucose measured during OGTT (A), fasting blood glucose (B), incremental area under the curve (AUC) (C), fasting plasma insulin (D) and plasma insulin levels after 15 minutes (E). Blood glucose levels during OGTT were analyzed by RM ANOVA. Data B-E were analyzed by one-way ANOVA with multiple comparison (uncorrected Fisher's LSD) of the mean of each experimental group. Results are presented as mean ± SEM. Statistical differences ($p \leq 0.05$) are marked by different letters.

3.4 White adipose tissue

3.4.1 Weight of WAT

At termination, selected adipose tissues and organs were harvested to investigate the impact of different diets on organ weight and adipocyte size. Weight of white adipose tissues are presented in figure 3.6. Liver weight, as well as weight of kidneys and *m. Tibialis anterior* are displayed in figure A.1 in appendix VI.

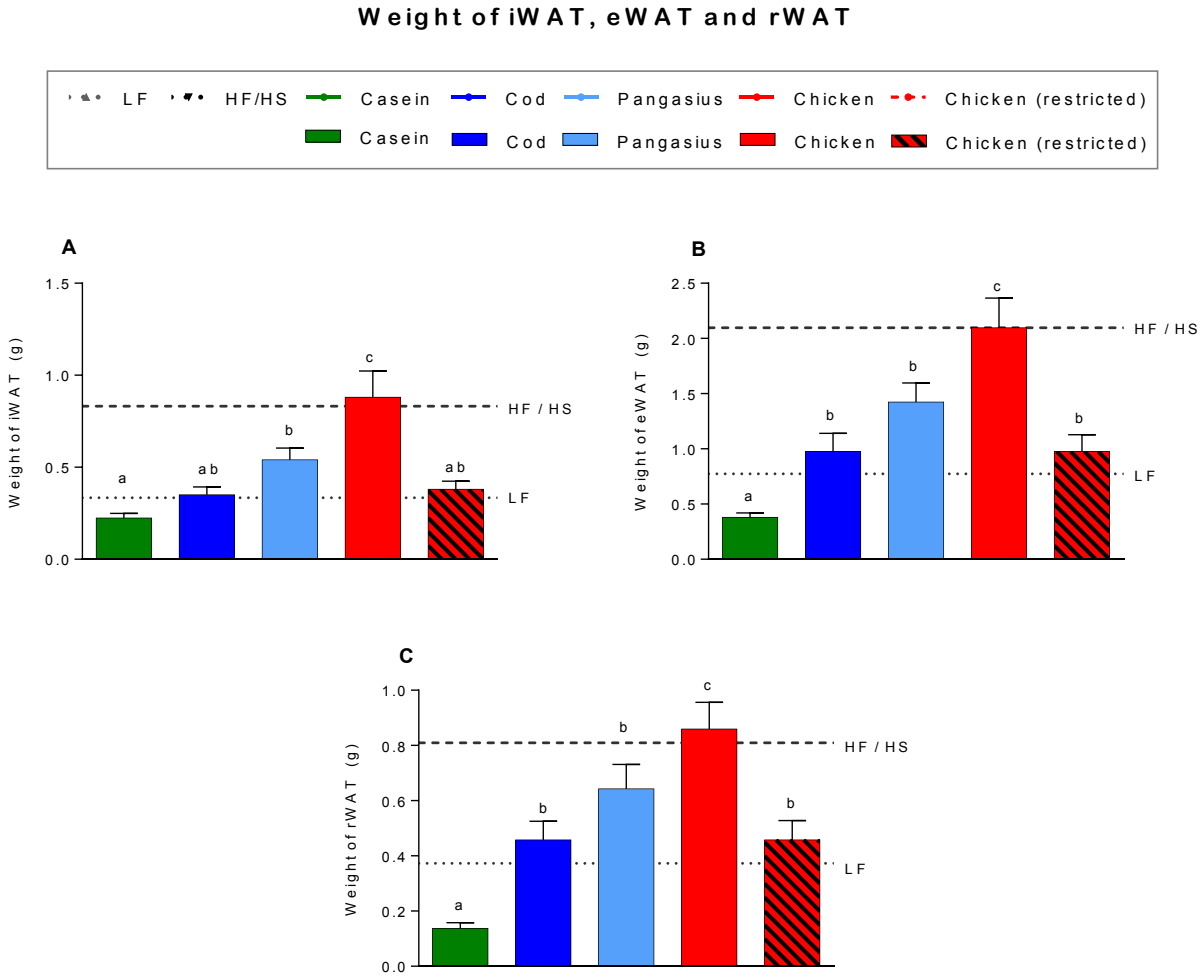

Figure 3.6 Weight of iWAT, eWAT and rWAT. Weigt of iWAT(A), eWAT(B) and rWAT(C) at termination. All data were analyzed by one-way ANOVA with multiple comparison (uncorrected Fisher's LSD) of the mean of each experimental group. Results are presented as mean ± SEM. Statistical differences ($p \leq 0.05$) are marked by different letters.

Naturally, weight of different adipose tissues appears to be associated with body weight. Mice fed casein had a significantly lower fat accumulation than all other groups in both eWAT and rWAT (figure 3.6 B-C). Further, pangasius and cod as protein sources promoted lower fat accumulation compared to chicken in all three WAT depots (figure 3.6 A-C). There was a trend towards an intermediate effect of pangasius, but no significant differences between this group and the one fed cod ($p = 0.08$ in all three depots).

3.4.2 Adipocyte size in iWAT

The adipocyte size in iWAT was examined by H&E staining of tissue sections, which was further studied by microscope and photographed. Mean adipocyte size was calculated by using Adiposoft. Results are shown in figure 3.7. The micrographs indicates that body weight development determines adipocyte size of iWAT. Differences in mean cell size between the two chicken-fed groups supports this. Large hypertrophic adipocytes can be observed in mice fed chicken, and mean adipocyte size in this group was similar to the HF/HS-fed reference group. Adipocyte size in mice fed pangasius was smaller and casein-fed mice had the smallest adipocytes, with the group fed cod in between.

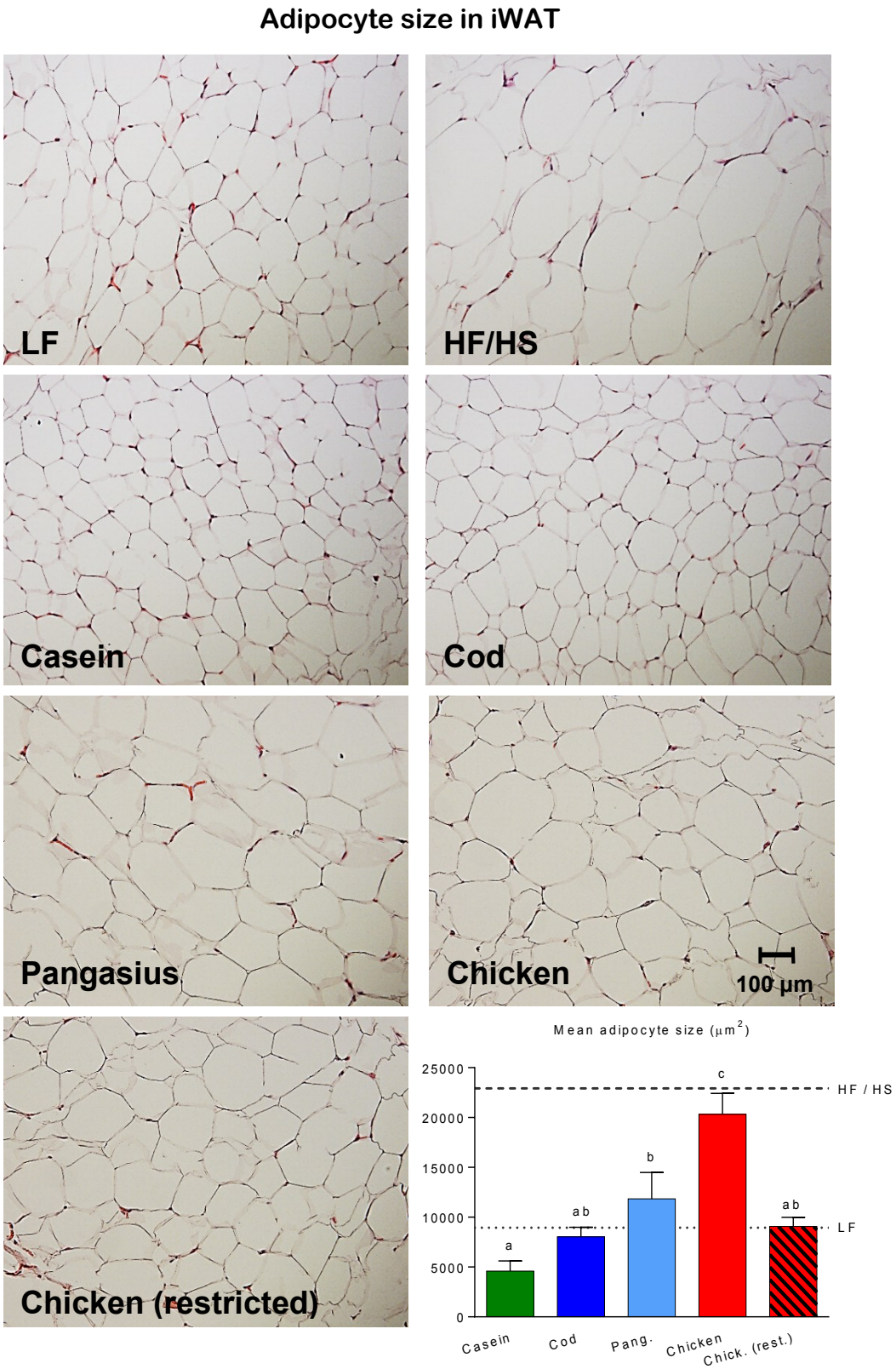

Figure 3.7 Adipocyte size in iWAT. Adipocyte micrographs of epididymal WAT (magnified x200) and mean adipocyte size. Mean adipocyte size was analyzed by one-way ANOVA with multiple comparison (uncorrected Fisher's LSD) of the mean. Results are presented as mean ± SEM. Statistical differences ($p \leq 0.05$) are marked by different letters.

3.5 Brown adipose tissue

Previous studies have observed a whitening of iBAT in mice fed chicken. To further investigate the whitening effect of different protein sources, H&E-staining and microscopy was carried out on sections of iBAT. BAT possess the ability to burn energy through thermogenesis and are consequently an important metabolic organ in mice. Hence, changes in BAT activity could affect energy expenditure and body weight gain. In order to investigate if such changes could be partially responsible for differences observed in feed efficiency, RT-qPCR and immunohistochemical staining of UCP1 was conducted.

3.5.1 Adipocyte size and weight of iBAT

Adipocyte size in iBAT were studied by staining and microscopy. Representative sections were photographed and are displayed in figure 3.8 along with weight of iBAT dissected at termination.

The micrographs illustrates a change in iBAT morphology, particularly in mice fed chicken and cod. In these groups, most brown adipocytes had changed from classical multilocular cells to unilocular ones (figure 3.8). The whitening effect of chicken appears to be attributable to greater iBAT- and body weight given that the mice fed chicken (restricted) had a more classic iBAT morphology. However, iBAT in the group fed pangasius had a more typical morphology compared to the one fed cod, despite higher body- and iBAT-weight (figure 3.8). Thus, lipid accumulation and whitening of iBAT was not solemnly body weight related.

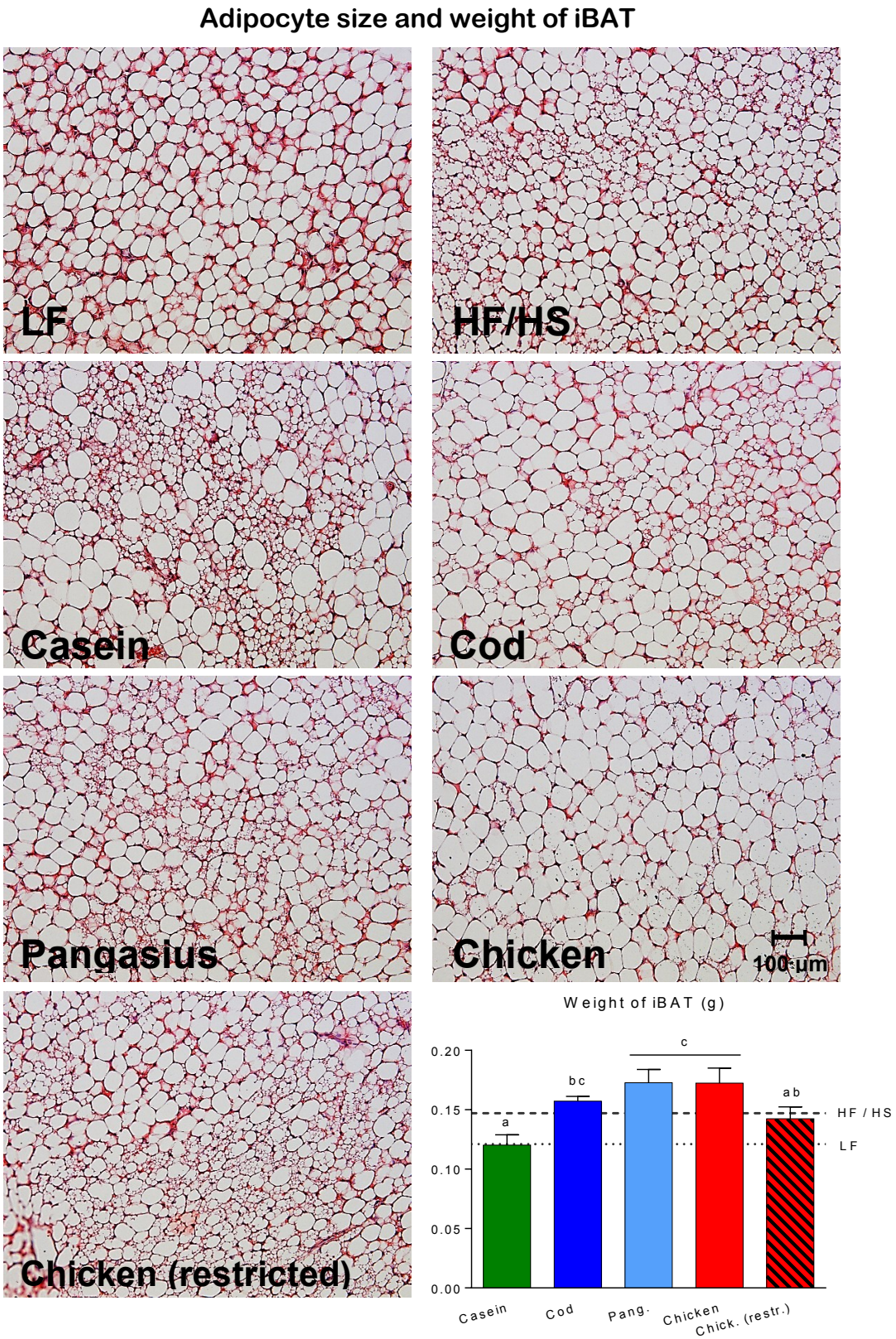

Figure 3.8 Adipocyte size and weight of iBAT. Adipocyte micrographs of interscapular BAT (magnified x200) and weight of iBAT at termination. iBAT weight was analyzed by one-way ANOVA with multiple comparison (uncorrected Fisher's LSD) of the mean. Results are presented as mean ± SEM. Statistical differences ($p \leq 0.05$) are marked by different letters.

3.5.2 Gene expression in iBAT

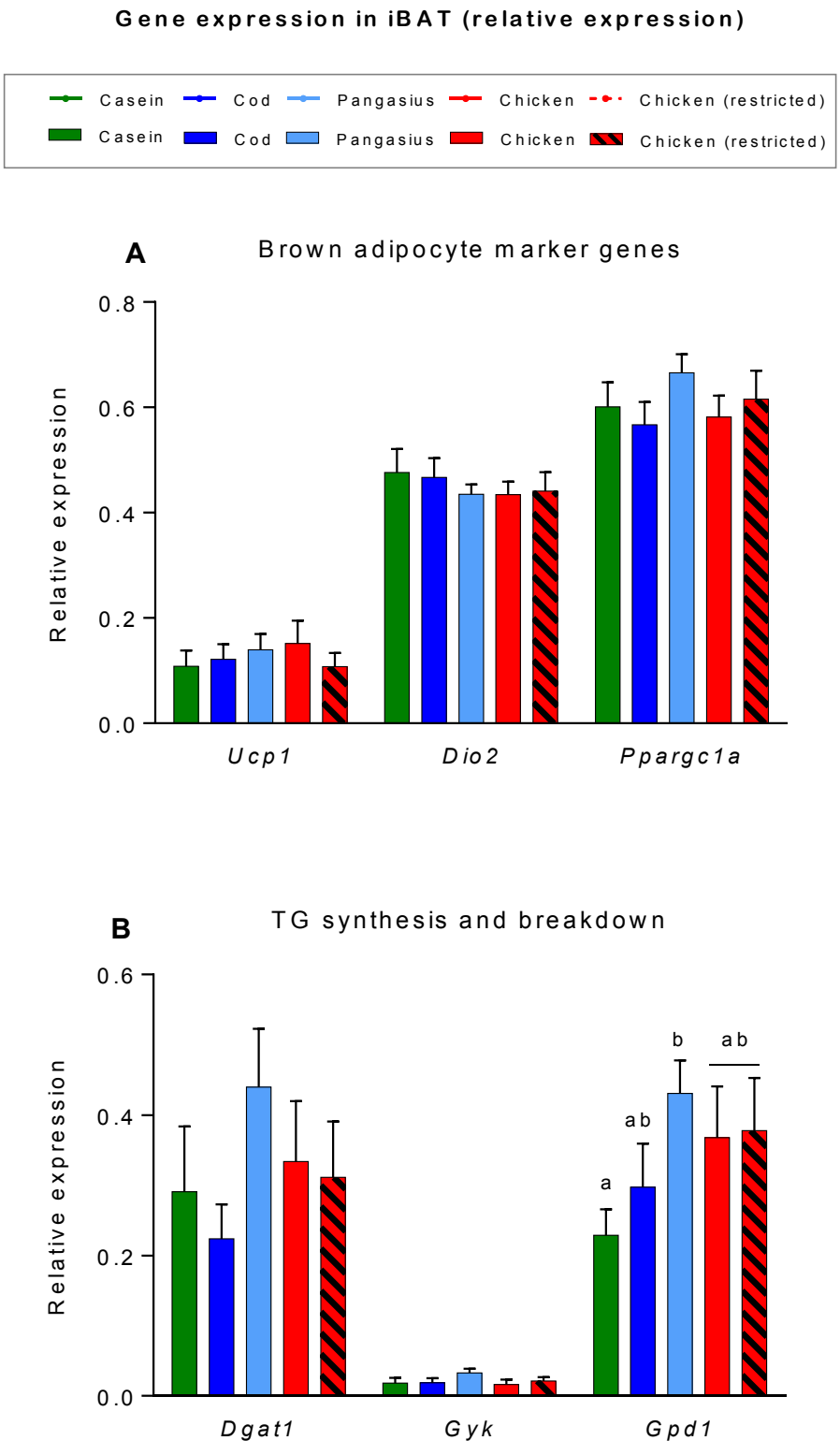

Figure 3.9 Gene expression in iBAT. Relative expression of genes associated with brown fat (A) and genes involved in triaglycerol synthesis and breakdown. Differences in gene expression were analyzed by one-way ANOVA with multiple comparison (uncorrected Fisher's LSD) of the mean. Results are presented as mean ± SEM. Statistical differences ($p \leq 0.05$) are marked by different letters.

RT-qPCR was used to study gene expression in iBAT (figure 3.9). Genes encoding the brown markers UCP1 (*Ucp1)*, iodothyorine deiodinase II (*Dio2)* and peroxisome proliferator-activated receptor gamma coactivator 1-alpha (*Ppargc1α*) was measured (figure 3.9 A). Expression levels of genes encoding diacylglycerol acyltransferase (*Dgat1)*, glycerol kinase (*Gyk*) and glycerol-3-phosphate dehydrogenase (*Gpd1)* was also determined (figure 3.9 B), the first protein is involved in TG synthesis whereas the two latter are active in TG breakdown.

Few significant differences were observed in gene expression. Expression of markers *Ucp1*, *Dio2* and *Ppargc1α* did not differ between the groups (figure 3.9 A), suggesting similar levels of metabolic activity in BAT. Elevated expression of genes involved in TG synthesis and breakdown could cause loss of energy through a futile cycling of FAs. Despite elevated expression of *Gpd1* in the pangasius-fed group compared to the one fed casein, no similar trends could be observed in expression of the other genes measured (figure 3.9 B).

3.5.3 Immunohistochemistry

mRNAs are a highly unstable components with a short half-life. Hence, differences in expression rate may not be detected by RT-qPCR due to rapid changes and degradation. In order to investigate expression of UCP1 on protein level, immunohistochemical staining of UCP1 in iBAT was performed, followed by microscopy. UCP1 expression was quantified by ImageJ, and results of microscopy and quantification are displayed in figure 3.10.

Higher expression of UCP1 was detected in the pangasius-fed group compared to the groups fed cod and chicken. Calorie restriction led to elevated expression of UCP1 in iBAT. Additionally, higher expression of the protein was detected in iBAT from mice fed casein compared to those fed chicken, but not those fed cod or chicken (restricted).

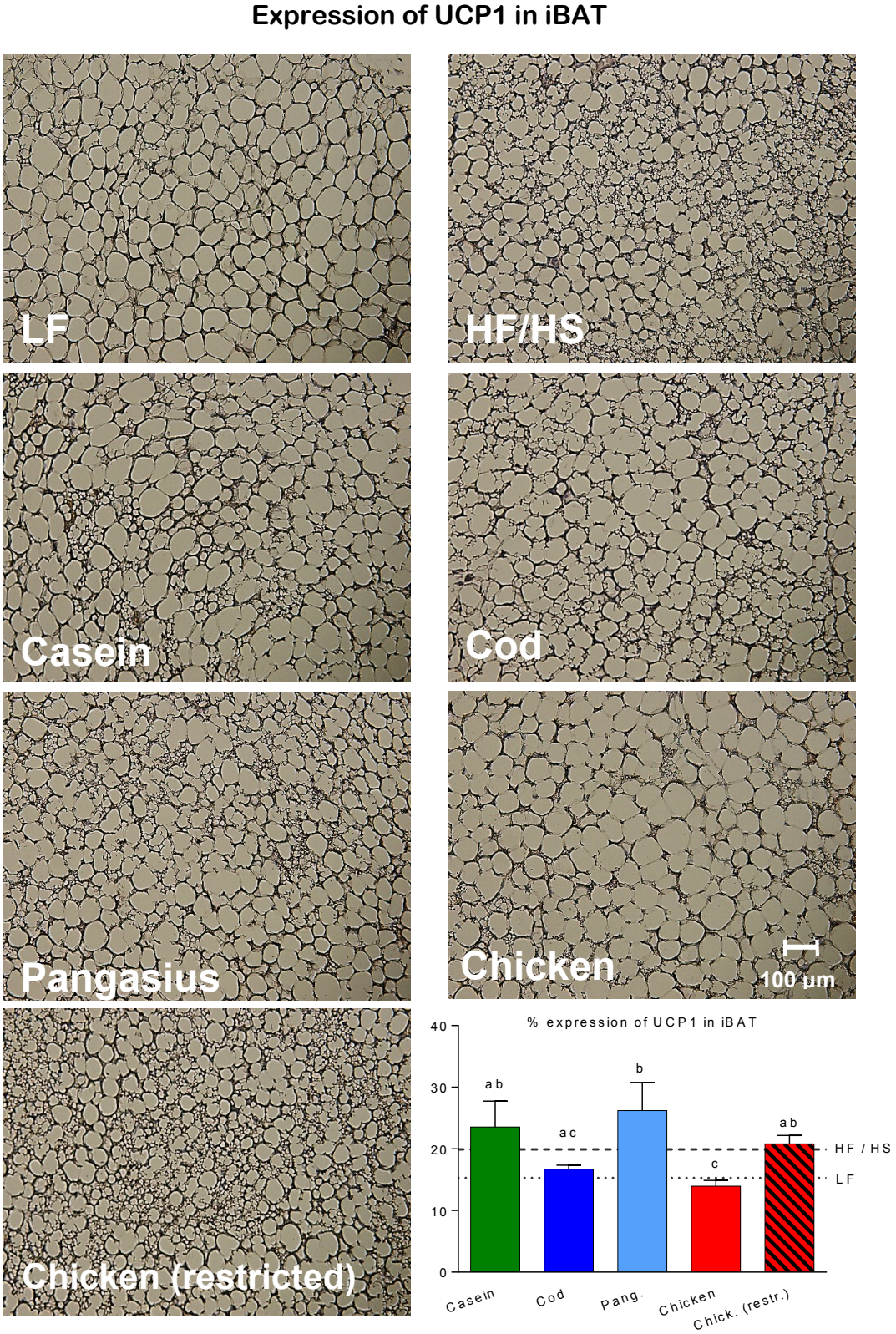

Figure 3.10 Expression of UCP1 in iBAT. Micrographs of immunohistochemically stained iBAT (magnified x200) and quantified UCP1 expression. Variations in UCP1 expression were analyzed by one-way ANOVA with multiple comparison (uncorrected Fisher's LSD) of the mean. Results are presented as mean ± SEM. Statistical differences ($p \leq 0.05$) are marked by different letters.

4.0 Discussion

In this study, we demonstrate that a HF/HP diet with pangasius as protein source has an intermediate effect on weight gain and fat accumulation compared to similar diets containing cod or chicken. This suggests that both amino acid composition and endogenous fat composition of the protein source affects the obesogenic potential of the diet. Further, we show that calorie restriction attenuates whitening of iBAT. Therefore, the whitening effect of chicken as a protein source seen in previous studies (Tastesen, Ronnevik, et al. 2014), seems to be a consequence of obesity rather than a cause. However, mice fed pangasius maintained a more classical iBAT morphology than those fed cod, despite higher body weight. iBAT morphology in mice fed pangasius were similar to casein-fed mice, suggesting that these protein sources might share an unknown factor which attenuates whitening of iBAT.

4.1 A HF/HP diet based on chicken is obesogenic relative to one based on cod, whereas a pangasius-based diet has an intermediate effect

4.1.1 Differences in body weight is partially caused by variations in energy intake

When given similar HP/HF diets containing either cod, pangasius or chicken, mice fed chicken had a significantly higher body weight gain compared to those fed cod. Mice fed pangasius gained more weight than the cod-fed mice, but less than those fed chicken. Moreover, calculated cumulative energy intake in the three different groups revealed a similar trend. Intake is highest in the chicken-fed group and lowest in the one fed cod, with the group fed pangasius in between, suggesting that differences in body weight may partly be due to differences in energy intake.

One possible explanation to the increased feed intake in the chicken-, and partially the pangasius-fed group, is elevated levels of endocannabinoids due to higher amounts of endogenous n-6 in the diet (table A.5, appendix I). Kirkham et al. (Kirkham et al. 2002) found that injections of 2-AG stimulated feeding in rats, supporting the theory that increased endocannabinoid signaling alters appetite regulation. Another study found that injection of AEA in satiated rats caused increased appetite (Jamshidi and Taylor 2001). Gomes et al. (Gomez et al. 2002) observed elevated AEA-levels in the small intestine of rats after fasting.

Moreover, when ECS was blocked using the CB1 antagonist rimonabant, feed intake decreased in fasted and partially satiated rats.

Increased appetite caused by elevated endocannabinoid signaling could explain why mice eat more of the n-6 rich chicken diet compared to the cod-based feed, which is lower in n-6 FAs. Further, the latter is also high in n-3 FAs, which might contribute to decreased ECS activation by lowering the amount of AA available for EC synthesis. When given to rats, a diet enriched with krill oil caused decreased concentrations of AEA and 2-AG in visceral adipose tissue and lower levels of AA in membrane phospholipids (Batetta et al. 2009). Alvheim et al. (Alvheim et al. 2012) also found that the adipogenic effect of a diet rich in LA was inhibited by consumption of EPA and DHA.

What the theory of increased EC-signaling does not explain, is the intermediate effect of the pangasius based diet on feed intake. This diet is rich in n-6 FAs and low in n-3, similar to the diet based on chicken. Still, the pangasius-fed mice had a lower energy intake compared to mice fed chicken. One possible explanation to this is the differences in amino acid composition between the two diets. A former study found that satiety was greater after ingestion of cod compared to chicken, and observed higher plasma levels of taurine after consumption of the fish meal (Uhe, Collier, and O'Dea 1992). In our study, the cod- and pangasius-based diets had higher levels of taurine relative to the one based on chicken. Tastesen et al. (Tastesen, Keenan, et al. 2014) showed that mice fed a HF/HS diet with scallop or crab, protein sources high in taurine, had a significantly lower feed intake compared to mice fed chicken. They further hypothesize that taurine in the diet might enhance the anorexigenic effects of insulin, resulting in lower energy intake. This is supported by another study in rats, where taurine supplementation in the drinking water resulted in decreased energy intake. Taurine-induced insulin signaling was also observed (Cappelli et al. 2014). It is important to notice that other studies have had contradictive results (Tsuboyama-Kasaoka et al. 2006).

Differences in palatability, caused by differences in amino acid composition, could also contribute to the differences in energy intake between cod-, pangasius- and chicken-fed mice. van Aavesaat et al. found that the taste of umami decreased subjective hunger and desire to eat compared to the taste of sweet or bitter (van Avesaat et al. 2015). The amino acid

glutamate is known to have an umami taste. Soup enriched with monosodium glutamate have been shown to reduce energy intake in women (Miyaki et al. 2016, Imada et al. 2014), suggesting that higher levels of glutamate in cod and pangasius could have a satiating effect. This is of course only speculation, as the effect of different amino acids on palatability is a field that requires more research.

As for the casein-based diet, elevated EC signaling due to high levels of n-6 FAs compared to n-3 FAs may partially account for the high energy intake. However, as this diet is high in glutamate, the high energy intake in this group is not in agreement with the theory of glutamate-induced satiety. It is worth noticing that the casein-diet had a slightly different texture, it was a "finer" powder, compared to the ones based on cod, pangasius and chicken. Furthermore, mice fed casein had a higher tendency to urinate in their food bowl. These are important aspects to consider when evaluating energy intake in the casein-fed group, since they made it harder to measure feed intake as accurately as in the other groups.

4.1.2 The protein- and fat source in the diet varied in their effect on feed efficiency

Interestingly, it seems that variations in energy intake is not the only reason for differences in body weight between the groups. The HF/HP diets also differ in their effect on feed efficiency. The chicken-based diet generates a higher feed efficiency than the one based on cod, whereas pangasius as protein source have an intermediate effect. Furthermore, analysis of apparent fat- and nitrogen digestibility makes it clear that the differences in feed efficiency is not due to varied absorption of nitrogen. As for apparent fat absorption, the cod-fed mice differ significantly from those fed chicken. Elevated fat excretion in this group may partially explain the differences in feed efficiency compared to the chicken-based diet. However, since the casein-fed mice have the highest apparent fat digestibility, elevated fat absorption does not explain the higher obesogenic effect of the chicken-based diet.

It seems that the ECS modulates energy expenditure as well as feed intake. Therefore, increased EC signaling may partially explain differences in feed efficiency as well as feed intake. An experiment by Cota et al. (Cota et al. 2003) showed that adult CB1 knockout mice had increased energy expenditure compared to wild type littermates. Decreased glucose uptake by muscle has also been suggested as a mechanism of which an overactive ESC reduces energy expenditure (Liu et al. 2005). In addition, it seems that activation of CB1

could stimulate PPAR-γ in mouse preadipocytes (Matias et al. 2006), an activation which has been shown to elevate feed efficiency in rats treated with PPAR-agonists (de Souza et al. 2001, Larsen et al. 2003).

Like the differences in feed intake, differences in feed efficiency can only partially be explained by impaired EC signaling. The intermediate effect of pangasius suggests that amino acid composition, as well as FA composition, affects feed efficiency. In mice fed a HF diet, taurine supplementation has been shown to elevate resting oxygen consumption, suggesting higher resting energy expenditure (Tsuboyama-Kasaoka et al. 2006). Moreover, Lin and colleagues observed lower body weight gain in mice fed a HF taurine enriched diet compared to a HF control group, despite pair feeding of the groups (Lin et al. 2013). Higher taurine content may therefore contribute to lower feed efficiency in the cod-based, and partially the pangasius-based diet.

When discussing feed efficiency, activity level is an important factor to consider. We did not do any measurements on activity level in this experiment. A previous study by our group found that mice fed pork had a tendency towards lower activity level compared to mice fed casein, although no significant differences were reported (Liisberg, Myrmel, et al. 2016). However, the differences in feed efficiency seen between the two chicken-fed groups suggests that higher feed efficiency due to lower activity levels is not caused by the protein source itself. Nonetheless, decreased physical activity due to high body weight could be a sort of vicious circle, enhancing the obesogenic effect of the diet.

The decreased feed efficiency in mice fed chicken (restricted) was a somewhat surprising discovery. Higher activity levels due to lower body weight could be part of the explanation. Further, it might be that the mice in this group received enough energy only to cover their basal metabolism, leaving no energy available for excess fat mass accumulation. Also, intermittent fasting is likely to alter metabolic processes, e.g. increase lipolysis (Tinsley and La Bounty 2015).

Increased energy expenditure due to higher thermogenesis in BAT would affect feed efficiency; this will be further discussed in section 4.2. Furthermore, differences in body composition, especially lean mass, ought to be considered.

4.1.3 Low lean mass in chicken-fed mice may increase feed efficiency

The MRI scan conducted in week nine revealed higher fat mass gain in the chicken-fed group compared to the group fed cod and pangasius. Further, the group fed pangasius had gained more fat than the one fed cod. Total fat mass was higher in mice fed chicken than mice fed cod, and there was a trend towards higher fat mass compared to pangasius-fed mice ($p = 0.09$). Adipose tissue functions as the main energy storage in vertebrates, thus a positive correlation between fat mass and body weight is natural. An *in vitro* study found that CB1 receptors are present in eWAT of C57BL/6N mice. Further, stimulation with a CB1 agonist dose-dependently increased lipoprotein lipase activity in these cells, showing that increased EC signaling may directly promote fat accumulation (Cota et al. 2003). However, this does not seem to be the case in our study. Micrographs of iWAT indicates that degree of hypotrophy in WAT adipocytes is determined by weight gain, not diet, as adipocyte size in iWAT of the calorie restricted group were similar to the one fed cod.

The casein- and cod-based diets seems superior to the one based on chicken regarding lean mass-gain. Of notice, obesity has been observed to cause increased intramuscular lipid storage (Goodpaster et al. 2000, Storlien et al. 1991), possibly resulting in slightly decreased muscle mass. Thus, decreased lean mass may be a consequence of weight gain. However, a similar trend can be observed in both obese and lean chicken-fed mice, suggesting that lean mass is not entirely decided by body weight. One possible explanation to the low lean mass in the group fed chicken (restricted) could be an elevated protein metabolism in order to compensate for the reduced energy intake. Nonetheless, this seems somewhat unlikely since energy intake in this group is similar to the one fed cod. Fasting may increase proteolysis, but short-term fasting periods (20-28 hours) does not appear to alter body protein metabolism (Tinsley and La Bounty 2015).

Lean mass, consisting mainly of muscle mass, is known to have higher metabolic activity compared with fat mass, and increased lean mass is associated with higher resting metabolic rate (Speakman and Selman 2003). It is therefore possible that observed differences in lean mass affects energy expenditure and that low lean mass in the chicken-fed group is a contributing factor to the high feed efficiency. The trend towards an intermediate effect of pangasius suggest that both amino acid composition and FA-composition of the diet affects lean mass development.

4.2 Body mass determines glucose tolerance and insulin sensitivity

Development of insulin resistance and diabetes type 2 are strongly related to overweight and obesity (WHO 2003). In concurrence with this, we observed impaired glucose tolerance and insulin sensitivity when body weight increased. RM ANOVA, revealing poor insulin response in the chicken- and pangasius-fed groups compared to the groups fed casein and chicken (restricted), supports this. High plasma insulin levels measured during OGTT show that despite little differences in AUC, the obese chicken fed mice have reduced inulin sensitivity compared with the other groups. Interestingly, while having the highest levels of fasting plasma insulin, the pangasius-fed group have similar plasma insulin levels as the cod- and casein-fed group fifteen minutes after glucose administration. Although explaining the high AUC of this group, it raises the question of why this group seems to have impaired glucose-stimulated insulin secretion.

Previous studies have suggested that taurine supplementation in obese mice improves glucose tolerance and insulin sensitivity (Batista et al. 2013, El Mesallamy et al. 2010). Notably, supplementation also attenuated body weight gain, underlining the close relationship between body weight gain and reduced insulin sensitivity. In concurrence with this, mice fed cod, the diet with the highest levels of taurine, have higher insulin sensitivity than mice fed chicken or pangasius. However, higher taurine content in the pangasius based diet compared with the one based on chicken did not seem to improve insulin sensitivity. Instead, in accordance with previous studies (Liisberg, Myrmel, et al. 2016), development of insulin resistance and glucose intolerance are consistent with increased body weight.

4.3 Calorie restriction attenuates whitening of iBAT, but changes are not solemnly decided by body weight

4.3.1 The whitening effect of chicken on iBAT morphology is weight related

One reason for including the calorie restricted chicken-fed group was to investigate whether the BAT-whitening effect of a chicken-based diet observed in previous studies is caused by the protein source, or rather a consequence of obesity. Micrographs reveals a classic morphology in iBAT of mice fed chicken (restricted) relative to those fed *ad libitum*, suggesting that whitening of iBAT is caused by weight gain. Similar observations was made

by Cinti et al. (Cinti et al. 1997), who further proposes low sympathetic stimulation as a possible cause. Sympathetic activation of BAT increases thermogenesis, and thus lipid consumption. Lowered sympathetic activity associated with obesity could therefore increase lipid accumulation in BAT (Cannon and Nedergaard 2004). Moreover, as discussed in section 4.1.2, obesity may cause decreased levels of physical activity. Higher activity levels in the mice fed chicken (restricted) could cause enhanced sympathetic stimulated thermogenesis in BAT, which may attenuate whitening.

Results from the two chicken-fed groups indicates that whitening of BAT is a consequence of obesity. However, lipid accumulation in iBAT was higher in cod-fed mice compared with those fed pangasius, despite lower body weight. This reveals the possible existence of other unknown factors, apart from obesity, that could either induce or attenuate BAT-whitening.

4.3.2 Pangasius attenuates obesity-induced whitening of iBAT

Micrographs of iBAT from mice fed casein, the group with the lowest body weight, shows a relatively classic BAT morphology. Ergo, casein as protein source either directly or through weight-regulating mechanisms, attenuates whitening of BAT. As stated in the previous section, micrographs of iBAT from mice fed pangasius implies that body weight alone does not determine the degree of whitening in BAT. Activation of PPAR-γ has been found to increase adipocyte size in BAT (Okamoto et al. 2007), offering one possible mechanism of BAT whitening. As previously discussed, increased EC activity has been observed to stimulate PPAR-γ in mice, meaning higher amounts of n-6 FAs in the diet could induce whitening of BAT. Furthermore, administration of the CB1 antagonist rimonabant resulted in decreased lipid droplet size in BAT from mice (Boon et al. 2014). Of notice, treatment with rimonabant also caused weight loss. The results from our study are clearly contradicting, given that the pangasius based diet contains high amounts of n-6 FAs. Another possible explanation for the differences observed in our experimental groups could be that whitening of iBAT in mice fed chicken, and to a lesser extent cod, are obesity related. Further, the pangasius- and casein-based diet share a similar unknown factor, possibly within their amino acid profile, that attenuates obesity-induced BAT whitening. One suggestion could be higher levels of BCAA. Nonetheless, the impact of different diets and amino acids on whitening of BAT is poorly understood and a topic that needs further exploration.

4.3.3 Increased iBAT activation is not the main cause of differences in feed efficiency

Few variations were observed in gene expression in iBAT. Elevated expression of *Gpd1* in mice fed pangasius relative to mice fed casein may suggest higher levels of TG breakdown. This is not reflected in body weight gain, as the pangasius-fed group had higher fat accumulation and body weight gain compared to the group fed cod. Given the short half-life of mRNA, the ability to detect differences in gene expression may get lost due to rapid degradation. In concurrence with this, immunohistochemical staining of UCP1 revealed significant differences in UCP1 expression on protein level. Amount of UCP1 in BAT appears to decrease with increased whitening of the tissue. Whether lower UCP1 levels and lower thermogenesis causes whitening or whitening causes lower amounts of UCP1 is unknown.

Since BAT is an important metabolic organ in mice, we hypothesized that variations observed in feed efficiency may be caused by changes in BAT activity. Further, we also speculated that such differences, if present, are attributable to differences in FA composition of the diets. The endocannabinoid system is believed to influence BAT activity, and administration of rimonabant to rats has been observed to increase expression of *Ucp1* in BAT (Verty, Allen, and Oldfield 2009). An increase in BAT temperature, indicating higher thermogenesis, was also observed. Boon and colleagues showed similar results in mice, where administration of rimonabant resulted in elevated *Ucp1* expression accompanied with more intense immunohistochemical staining of UCP1 (Boon et al. 2014). Surprisingly, in our study highest amounts of UCP1 was found not only in the lean casein- and chicken (restricted)-fed mice, but also in mice fed pangasius. This does not reject the theory that elevated EC signaling, due to increased intake of n-6 FA, decreases thermogenesis in BAT. However, it highlights the existence of yet unknown diet-induced countervailing mechanisms.

4.4 The animal model and relevance to humans

This is an animal study, and it is important to state that the results of this study cannot be directly applied to humans. However, human studies are far more expensive and time consuming to conduct. Additionally, such studies offer many ethical limitations and a human environment is far less controllable compared to that of animals. Hence, animal studies are an important part of basic nutritional research and results from such studies may give valuable information on biological mechanisms.

Mice are one of the most commonly used animal models in nutritional research since they are similar to humans both genetically and physiologically. Of notice, mice used for animal research are usually from inbred strains, which have less genetic variations than humans do. As previously stated, the C57BL/6J mouse model used in this experiment is characterized by its ability to develop obesity, hyperglycemia and hyperinsulinemia when fed a HF diet. It is therefore a suitable model for studying the pathophysiology of obesity, undergoing similar changes as the ones observed in humans. The monotonous mouse diets in this experiment are very different from a varied human food intake. However, in concordance with an increased focus on food and dietary patterns rather than single isolated nutrients (Mozaffarian 2016, Helsedirektoratet 2014), the main focus in our experiment was natural protein sources rather than protein powder or hydrolyzed protein.

4.5 Future perspectives

We observed an elevated feed intake in mice fed the chicken-based diet compared to those fed cod, with an intermediate effect when pangasius was used as protein source. Altered EC signaling could cause such variations. In order to draw any conclusions on whether this may be the case in our study, analysis of endocannabinoid levels in tissues and/or plasma are essential. Analysis of amino acids in plasma could also be of use, as this may reveal similarities/differences in the cod- and pangasius-based diet compared to the one based on chicken and help elaborate the importance and effect of the different amino acids.

In this study, we focused on changes in BAT. We cannot exclude the possibility that different diets induced formation of brown or beige adipocytes in WAT. Such changes could affect energy expenditure and contribute to the variations observed in feed efficiency. A RT-qPCR analysis of *Ucp1* expression and other brown markers in WAT could therefore be of relevance. Further, histology and analysis of gene expression in liver may be of interest, as liver steatosis, obesity and insulin resistance are closely related. Investigations on gut microbiota could also be conducted since duodenum, jejunum, ileum and colon were harvested at termination.

Diet-induced obesity was observed in mice fed a HF/HP diet based on chicken, and to some degree pangasius, relative to similar diets based on casein and cod. Carbohydrate content was similar in all three diets. It would be interesting to see if mice still develops obesity when fed a HF/HP diet if the carbohydrates are changed from sugar and starch to carbohydrates with lower glycemic index. To study the obesogenic effect of different protein sources in other diets, such as a LF diet or a HF/HS diet may also be of use.

Last but not least, it would be of great importance to investigate if similar results can be observed in human studies.

5.0 Conclusion

The obesogenic effect of a HF/HP diet in C57BL/6J mice is contingent upon the protein source used. Chicken as protein source are obesogenic relative to cod, whereas pangasius has an intermediate effect. Thus, it appears both FA- and amino acid composition determines the obesogenic effect of HF/HP diets. Further, various HF/HP diets differ in impact on iBAT morphology and levels of UCP1. Calorie restriction attenuates this, but type of protein source used is also a determining factor. Protein from pangasius and casein appears expedient in this context, and so diversities in body weight gain are not solemnly attributable to altered appearance and activity in BAT. Body weight appears to be the main determining factor in development of insulin resistance.

To understand the underlying mechanisms responsible for the unequal obesogenic potential of different proteins, further research is required. Since high protein diets are popular methods of weight management and weight loss in humans, results from this study also highlight the value of further research to explore the obesogenic effect of different proteins in human nutrition.

REFERENCES

Alvheim, A. R., M. K. Malde, D. Osei-Hyiaman, Y. H. Lin, R. J. Pawlosky, L. Madsen, K. Kristiansen, L. Froyland, and J. R. Hibbeln. 2012. "Dietary linoleic acid elevates endogenous 2-AG and anandamide and induces obesity." *Obesity (Silver Spring)* 20 (10):1984-94. doi: 10.1038/oby.2012.38.

Batetta, B., M. Griinari, G. Carta, E. Murru, A. Ligresti, L. Cordeddu, E. Giordano, F. Sanna, T. Bisogno, S. Uda, M. Collu, I. Bruheim, V. Di Marzo, and S. Banni. 2009. "Endocannabinoids may mediate the ability of (n-3) fatty acids to reduce ectopic fat and inflammatory mediators in obese Zucker rats." *J Nutr* 139 (8):1495-501. doi: 10.3945/jn.109.104844.

Batista, T. M., R. A. Ribeiro, P. M. da Silva, R. L. Camargo, P. C. Lollo, A. C. Boschero, and E. M. Carneiro. 2013. "Taurine supplementation improves liver glucose control in normal protein and malnourished mice fed a high-fat diet." *Mol Nutr Food Res* 57 (3):423-34. doi: 10.1002/mnfr.201200345.

Bere, E.; Øverby, N.C. 2011. "Energi." In *Om mat og ernæring*, page 34. Kristiansand: Høyskoleforlaget AS.

Black, B. L., J. Croom, E. J. Eisen, A. E. Petro, C. L. Edwards, and R. S. Surwit. 1998. "Differential effects of fat and sucrose on body composition in A/J and C57BL/6 mice." *Metabolism* 47 (11):1354-9.

Blasbalg, T. L., J. R. Hibbeln, C. E. Ramsden, S. F. Majchrzak, and R. R. Rawlings. 2011. "Changes in consumption of omega-3 and omega-6 fatty acids in the United States during the 20th century." *Am J Clin Nutr* 93 (5):950-62. doi: 10.3945/ajcn.110.006643.

Boon, M. R., S. Kooijman, A. D. van Dam, L. R. Pelgrom, J. F. Berbee, C. A. Visseren, R. C. van Aggele, A. M. van den Hoek, H. C. Sips, M. Lombes, L. M. Havekes, J. T. Tamsma, B. Guigas, O. C. Meijer, J. W. Jukema, and P. C. Rensen. 2014. "Peripheral cannabinoid 1 receptor blockade activates brown adipose tissue and diminishes dyslipidemia and obesity." *Faseb j* 28 (12):5361-75. doi: 10.1096/fj.13-247643.

Cannon, B., and J. Nedergaard. 2004. "Brown adipose tissue: function and physiological significance." *Physiol Rev* 84 (1):277-359. doi: 10.1152/physrev.00015.2003.

Cappelli, A. P., C. C. Zoppi, H. C. Barbosa-Sampaio, J. M. Costa, Jr., A. O. Protzek, P. N. Morato, A. C. Boschero, and E. M. Carneiro. 2014. "Taurine-induced insulin signalling improvement of obese malnourished mice is associated with redox balance and protein phosphatases activity modulation." *Liver Int* 34 (5):771-83. doi: 10.1111/liv.12291.

Cinti, S. 2009. "Transdifferentiation properties of adipocytes in the adipose organ." *Am J Physiol Endocrinol Metab* 297 (5):E977-86. doi: 10.1152/ajpendo.00183.2009.

Cinti, S., R. C. Frederich, M. C. Zingaretti, R. De Matteis, J. S. Flier, and B. B. Lowell. 1997. "Immunohistochemical localization of leptin and uncoupling protein in white and brown adipose tissue." *Endocrinology* 138 (2):797-804. doi: 10.1210/endo.138.2.4908.

Cota, D., G. Marsicano, M. Tschop, Y. Grubler, C. Flachskamm, M. Schubert, D. Auer, A. Yassouridis, C. Thone-Reineke, S. Ortmann, F. Tomassoni, C. Cervino, E. Nisoli, A. C. Linthorst, R. Pasquali, B. Lutz, G. K. Stalla, and U. Pagotto. 2003. "The endogenous cannabinoid system affects energy balance via central orexigenic drive and peripheral lipogenesis." *J Clin Invest* 112 (3):423-31. doi: 10.1172/jci17725.

Cypess, A. M., S. Lehman, G. Williams, I. Tal, D. Rodman, A. B. Goldfine, F. C. Kuo, E. L. Palmer, Y. H. Tseng, A. Doria, G. M. Kolodny, and C. R. Kahn. 2009. "Identification and importance of brown adipose tissue in adult humans." *N Engl J Med* 360 (15):1509-17. doi: 10.1056/NEJMoa0810780.

de Lorgeril, M., and P. Salen. 2012. "New insights into the health effects of dietary saturated and omega-6 and omega-3 polyunsaturated fatty acids." *BMC Med* 10:50. doi: 10.1186/1741-7015-10-50.

de Souza, C. J., M. Eckhardt, K. Gagen, M. Dong, W. Chen, D. Laurent, and B. F. Burkey. 2001. "Effects of pioglitazone on adipose tissue remodeling within the setting of obesity and insulin resistance." *Diabetes* 50 (8):1863-71.

El Mesallamy, H. O., E. El-Demerdash, L. N. Hammad, and H. M. El Magdoub. 2010. "Effect of taurine supplementation on hyperhomocysteinemia and markers of oxidative stress in high fructose diet induced insulin resistance." *Diabetol Metab Syndr* 2:46. doi: 10.1186/1758-5996-2-46.

FAO. 2010. "Fats and fatty acids in human nutrition." Food and Agriculture Organization of the United Nations, Accessed 03.16.16. http://www.who.int/nutrition/publications/nutrientrequirements/fatsandfattyacids_humannutrition/en/.

FAO. 2013. "The State of Food and Agriculture." Food and Agriculture Organization of the United Nations Accessed 01.13.16. http://www.fao.org/docrep/018/i3300e/i3300e.pdf.

Fruhbeck, G., J. Gomez-Ambrosi, F. J. Muruzabal, and M. A. Burrell. 2001. "The adipocyte: a model for integration of endocrine and metabolic signaling in energy metabolism regulation." *Am J Physiol Endocrinol Metab* 280 (6):E827-47.

Galarraga, M., J. Campion, A. Munoz-Barrutia, N. Boque, H. Moreno, J. A. Martinez, F. Milagro, and C. Ortiz-de-Solorzano. 2012. "Adiposoft: automated software for the analysis of white adipose tissue cellularity in histological sections." *J Lipid Res* 53 (12):2791-6. doi: 10.1194/jlr.D023788.

Gerrior, S., Bente, L. & Hiza, H. 2004. Nutrient Content of the U.S. Food Supply, 1909-2000. (Home Economics Research Report No. 56). U.S. Department of Agriculture, Center for Nutrition Policy and Promotion.

Gilbert, J. A., N. T. Bendsen, A. Tremblay, and A. Astrup. 2011. "Effect of proteins from different sources on body composition." *Nutr Metab Cardiovasc Dis* 21 Suppl 2:B16-31. doi: 10.1016/j.numecd.2010.12.008.

Gomez, R., M. Navarro, B. Ferrer, J. M. Trigo, A. Bilbao, I. Del Arco, A. Cippitelli, F. Nava, D. Piomelli, and F. Rodriguez de Fonseca. 2002. "A peripheral mechanism for CB1 cannabinoid receptor-dependent modulation of feeding." *J Neurosci* 22 (21):9612-7.

Goodpaster, B. H., R. Theriault, S. C. Watkins, and D. E. Kelley. 2000. "Intramuscular lipid content is increased in obesity and decreased by weight loss." *Metabolism* 49 (4):467-72.

Goyens, P. L., M. E. Spilker, P. L. Zock, M. B. Katan, and R. P. Mensink. 2006. "Conversion of alpha-linolenic acid in humans is influenced by the absolute amounts of alpha-linolenic acid and linoleic acid in the diet and not by their ratio." *Am J Clin Nutr* 84 (1):44-53.

Halton, T. L., and F. B. Hu. 2004. "The effects of high protein diets on thermogenesis, satiety and weight loss: a critical review." *J Am Coll Nutr* 23 (5):373-85.

Harris, W. S. 2006. "The omega-6/omega-3 ratio and cardiovascular disease risk: uses and abuses." *Curr Atheroscler Rep* 8 (6):453-9.

Harris, W. S., B. Assaad, and W. C. Poston. 2006. "Tissue omega-6/omega-3 fatty acid ratio and risk for coronary artery disease." *Am J Cardiol* 98 (4a):19i-26i. doi: 10.1016/j.amjcard.2005.12.023.

Helsedirektoratet. 2014. Anbefalinger om kosthold, ernæring og fysisk aktivitet.

Himms-Hagen, J., A. Melnyk, M. C. Zingaretti, E. Ceresi, G. Barbatelli, and S. Cinti. 2000. "Multilocular fat cells in WAT of CL-316243-treated rats derive directly from white adipocytes." *Am J Physiol Cell Physiol* 279 (3):C670-81.

Imada, T., S. S. Hao, K. Torii, and E. Kimura. 2014. "Supplementing chicken broth with monosodium glutamate reduces energy intake from high fat and sweet snacks in middle-aged healthy women." *Appetite* 79:158-65. doi: 10.1016/j.appet.2014.04.011.

Jamshidi, N., and D. A. Taylor. 2001. "Anandamide administration into the ventromedial hypothalamus stimulates appetite in rats." *Br J Pharmacol* 134 (6):1151-4. doi: 10.1038/sj.bjp.0704379.

Johnson, G. H., and K. Fritsche. 2012. "Effect of dietary linoleic acid on markers of inflammation in healthy persons: a systematic review of randomized controlled trials." *J Acad Nutr Diet* 112 (7):1029-41, 1041.e1-15. doi: 10.1016/j.jand.2012.03.029.

Kim, J., Y. Li, and B. A. Watkins. 2011. "Endocannabinoid signaling and energy metabolism: a target for dietary intervention." *Nutrition* 27 (6):624-32. doi: 10.1016/j.nut.2010.11.003.

Kirkham, T. C., C. M. Williams, F. Fezza, and V. Di Marzo. 2002. "Endocannabinoid levels in rat limbic forebrain and hypothalamus in relation to fasting, feeding and satiation: stimulation of eating by 2-arachidonoyl glycerol." *Br J Pharmacol* 136 (4):550-7. doi: 10.1038/sj.bjp.0704767.

Kyrou, I., H. S. Randeva, and M. O. Weickert. 2000. "Clinical Problems Caused by Obesity." In *Endotext*, edited by L. J. De Groot, P. Beck-Peccoz, G. Chrousos, K. Dungan, A. Grossman, J. M. Hershman, C. Koch, R. McLachlan, M. New, R. Rebar, F. Singer, A. Vinik and M. O. Weickert. South Dartmouth (MA): MDText.com, Inc.

Larsen, P. J., P. B. Jensen, R. V. Sorensen, L. K. Larsen, N. Vrang, E. M. Wulff, and K. Wassermann. 2003. "Differential influences of peroxisome proliferator-activated receptors gamma and -alpha on food intake and energy homeostasis." *Diabetes* 52 (9):2249-59.

Leidy, H. J., N. S. Carnell, R. D. Mattes, and W. W. Campbell. 2007. "Higher protein intake preserves lean mass and satiety with weight loss in pre-obese and obese women." *Obesity (Silver Spring)* 15 (2):421-9. doi: 10.1038/oby.2007.531.

Ley, R. E., P. J. Turnbaugh, S. Klein, and J. I. Gordon. 2006. "Microbial ecology: human gut microbes associated with obesity." *Nature* 444 (7122):1022-3. doi: 10.1038/4441022a.

Liisberg, U., K. R. Fauske, O. Kuda, E. Fjaere, L. S. Myrmel, N. Norberg, L. Froyland, I. E. Graff, B. Liaset, K. Kristiansen, J. Kopecky, and L. Madsen. 2016. "Intake of a Western diet containing cod instead of pork alters fatty acid composition in tissue phospholipids and attenuates obesity and hepatic lipid accumulation in mice." *J Nutr Biochem* 33:119-127. doi: 10.1016/j.jnutbio.2016.03.014.

Liisberg, Ulrike, Lene Secher Myrmel, Even Fjære, Alexander K. Rønnevik, Susanne Bjelland, Kristin Røen Fauske, Jacob Bak Holm, Astrid Linde Basse, Jacob B. Hansen, Bjørn Liaset, Karsten Kristiansen, and Lise Madsen. 2016. "The protein source determines the potential of high protein diets to attenuate obesity development in C57BL/6J mice." *Adipocyte*:1-16. doi: 10.1080/21623945.2015.1122855.

Lin, S., S. Hirai, Y. Yamaguchi, T. Goto, N. Takahashi, F. Tani, C. Mutoh, T. Sakurai, S. Murakami, R. Yu, and T. Kawada. 2013. "Taurine improves obesity-induced inflammatory responses and modulates the unbalanced phenotype of adipose tissue macrophages." *Mol Nutr Food Res* 57 (12):2155-65. doi: 10.1002/mnfr.201300150.

Liu, Y. L., I. P. Connoley, C. A. Wilson, and M. J. Stock. 2005. "Effects of the cannabinoid CB1 receptor antagonist SR141716 on oxygen consumption and soleus muscle glucose uptake in Lep(ob)/Lep(ob) mice." *Int J Obes (Lond)* 29 (2):183-7. doi: 10.1038/sj.ijo.0802847.

Loncar, D., B. A. Afzelius, and B. Cannon. 1988. "Epididymal white adipose tissue after cold stress in rats. I. Nonmitochondrial changes." *J Ultrastruct Mol Struct Res* 101 (2-3):109-22.

Lucan, S. C., and J. J. DiNicolantonio. 2015. "How calorie-focused thinking about obesity and related diseases may mislead and harm public health. An alternative." *Public Health Nutr* 18 (4):571-81. doi: 10.1017/s1368980014002559.

Matias, I., and V. Di Marzo. 2007. "Endocannabinoids and the control of energy balance." *Trends Endocrinol Metab* 18 (1):27-37. doi: 10.1016/j.tem.2006.11.006.

Matias, I., M. P. Gonthier, P. Orlando, V. Martiadis, L. De Petrocellis, C. Cervino, S. Petrosino, L. Hoareau, F. Festy, R. Pasquali, R. Roche, M. Maj, U. Pagotto, P. Monteleone, and V. Di Marzo. 2006. "Regulation, function, and dysregulation of endocannabinoids in models of adipose and beta-pancreatic cells and in obesity and hyperglycemia." *J Clin Endocrinol Metab* 91 (8):3171-80. doi: 10.1210/jc.2005-2679.

Miyaki, T., T. Imada, S. S. Hao, and E. Kimura. 2016. "Monosodium L-glutamate in soup reduces subsequent energy intake from high-fat savoury food in overweight and obese women." *Br J Nutr* 115 (1):176-84. doi: 10.1017/s0007114515004031.

Mozaffarian, D. 2016. "Dietary and Policy Priorities for Cardiovascular Disease, Diabetes, and Obesity: A Comprehensive Review." *Circulation* 133 (2):187-225. doi: 10.1161/circulationaha.115.018585.

O'Rahilly, S., and I. S. Farooqi. 2000. "The Genetics of Obesity in Humans." In *Endotext*, edited by L. J. De Groot, P. Beck-Peccoz, G. Chrousos, K. Dungan, A. Grossman, J. M. Hershman, C. Koch, R. McLachlan, M. New, R. Rebar, F. Singer, A. Vinik and M. O. Weickert. South Dartmouth (MA): MDText.com, Inc.

Okamoto, Y., H. Higashiyama, H. Inoue, M. Kanematsu, M. Kinoshita, and S. Asano. 2007. "Quantitative image analysis in adipose tissue using an automated image analysis system: differential effects of peroxisome proliferator-activated receptor-alpha and -gamma agonist on white and brown adipose tissue morphology in AKR obese and db/db diabetic mice." *Pathol Int* 57 (6):369-77. doi: 10.1111/j.1440-1827.2007.02109.x.

Peirce, V., S. Carobbio, and A. Vidal-Puig. 2014. "The different shades of fat." *Nature* 510 (7503):76-83. doi: 10.1038/nature13477.

Poekes, L., N. Lanthier, and I. A. Leclercq. 2015. "Brown adipose tissue: a potential target in the fight against obesity and the metabolic syndrome." *Clin Sci (Lond)* 129 (11):933-49. doi: 10.1042/cs20150339.

Rodriguez, A., S. Ezquerro, L. Mendez-Gimenez, S. Becerril, and G. Fruhbeck. 2015. "Revisiting the adipocyte: a model for integration of cytokine signaling in the regulation of energy metabolism." *Am J Physiol Endocrinol Metab* 309 (8):E691-714. doi: 10.1152/ajpendo.00297.2015.

Rosenwald, M., A. Perdikari, T. Rulicke, and C. Wolfrum. 2013. "Bi-directional interconversion of brite and white adipocytes." *Nat Cell Biol* 15 (6):659-67. doi: 10.1038/ncb2740.

Rossmeisl, M., Z. M. Jilkova, O. Kuda, T. Jelenik, D. Medrikova, B. Stankova, B. Kristinsson, G. G. Haraldsson, H. Svensen, I. Stoknes, P. Sjovall, Y. Magnusson, M. G. Balvers, K. C. Verhoeckx, E. Tvrzicka, M. Bryhn, and J. Kopecky. 2012. "Metabolic effects of n-3 PUFA as phospholipids are superior to triglycerides in mice fed a high-fat diet: possible role of endocannabinoids." *PLoS One* 7 (6):e38834. doi: 10.1371/journal.pone.0038834.

Russo, G. L. 2009. "Dietary n-6 and n-3 polyunsaturated fatty acids: from biochemistry to clinical implications in cardiovascular prevention." *Biochem Pharmacol* 77 (6):937-46. doi: 10.1016/j.bcp.2008.10.020.

Sanchez-Gurmaches, J., C. M. Hung, C. A. Sparks, Y. Tang, H. Li, and D. A. Guertin. 2012. "PTEN loss in the Myf5 lineage redistributes body fat and reveals subsets of white adipocytes that arise from Myf5 precursors." *Cell Metab* 16 (3):348-62. doi: 10.1016/j.cmet.2012.08.003.

Seale, P., B. Bjork, W. Yang, S. Kajimura, S. Chin, S. Kuang, A. Scime, S. Devarakonda, H. M. Conroe, H. Erdjument-Bromage, P. Tempst, M. A. Rudnicki, D. R. Beier, and B. M. Spiegelman. 2008. "PRDM16 controls a brown fat/skeletal muscle switch." *Nature* 454 (7207):961-7. doi: 10.1038/nature07182.

Simopoulos, A. P. 1999. "Essential fatty acids in health and chronic disease." *Am J Clin Nutr* 70 (3 Suppl):560s-569s.

Simopoulos, A. P. 2002. "The importance of the ratio of omega-6/omega-3 essential fatty acids." *Biomed Pharmacother* 56 (8):365-79.

Simopoulos, A. P. 2016. "An Increase in the Omega-6/Omega-3 Fatty Acid Ratio Increases the Risk for Obesity." *Nutrients* 8 (3). doi: 10.3390/nu8030128.

Speakman, J. R., and C. Selman. 2003. "Physical activity and resting metabolic rate." *Proc Nutr Soc* 62 (3):621-34. doi: 10.1079/pns2003282.

Storlien, L. H., A. B. Jenkins, D. J. Chisholm, W. S. Pascoe, S. Khouri, and E. W. Kraegen. 1991. "Influence of dietary fat composition on development of insulin resistance in rats. Relationship to muscle triglyceride and omega-3 fatty acids in muscle phospholipid." *Diabetes* 40 (2):280-9.

Surwit, R. S., C. M. Kuhn, C. Cochrane, J. A. McCubbin, and M. N. Feinglos. 1988. "Diet-induced type II diabetes in C57BL/6J mice." *Diabetes* 37 (9):1163-7.

Tappy, L. 1996. "Thermic effect of food and sympathetic nervous system activity in humans." *Reprod Nutr Dev* 36 (4):391-7.

Tastesen, H. S., A. H. Keenan, L. Madsen, K. Kristiansen, and B. Liaset. 2014. "Scallop protein with endogenous high taurine and glycine content prevents high-fat, high-sucrose-induced obesity and improves plasma lipid profile in male C57BL/6J mice." *Amino Acids* 46 (7):1659-71. doi: 10.1007/s00726-014-1715-1.

Tastesen, H. S., A. K. Ronnevik, K. Borkowski, L. Madsen, K. Kristiansen, and B. Liaset. 2014. "A mixture of cod and scallop protein reduces adiposity and improves glucose tolerance in high-fat fed male C57BL/6J mice." *PLoS One* 9 (11):e112859. doi: 10.1371/journal.pone.0112859.

Taubes, G. 2010. *Why We Get Fat: And What To Do About It*. New York, USA: Alfred A. Knopf.

Te Morenga, L., and J. Mann. 2012. "The role of high-protein diets in body weight management and health." *Br J Nutr* 108 Suppl 2:S130-8. doi: 10.1017/s0007114512002437.
Tinsley, G. M., and P. M. La Bounty. 2015. "Effects of intermittent fasting on body composition and clinical health markers in humans." *Nutr Rev* 73 (10):661-74. doi: 10.1093/nutrit/nuv041.
Tsuboyama-Kasaoka, N., C. Shozawa, K. Sano, Y. Kamei, S. Kasaoka, Y. Hosokawa, and O. Ezaki. 2006. "Taurine (2-aminoethanesulfonic acid) deficiency creates a vicious circle promoting obesity." *Endocrinology* 147 (7):3276-84. doi: 10.1210/en.2005-1007.
Uhe, A. M., G. R. Collier, and K. O'Dea. 1992. "A comparison of the effects of beef, chicken and fish protein on satiety and amino acid profiles in lean male subjects." *J Nutr* 122 (3):467-72.
van Avesaat, M., F. J. Troost, D. Ripken, J. Peters, H. F. Hendriks, and A. A. Masclee. 2015. "Intraduodenal infusion of a combination of tastants decreases food intake in humans." *Am J Clin Nutr* 102 (4):729-35. doi: 10.3945/ajcn.115.113266.
van Dam, R. M., and J. C. Seidell. 2007. "Carbohydrate intake and obesity." *Eur J Clin Nutr* 61 Suppl 1:S75-99. doi: 10.1038/sj.ejcn.1602939.
Verty, A. N., A. M. Allen, and B. J. Oldfield. 2009. "The effects of rimonabant on brown adipose tissue in rat: implications for energy expenditure." *Obesity (Silver Spring)* 17 (2):254-61. doi: 10.1038/oby.2008.509.
Virtanen, K. A., M. E. Lidell, J. Orava, M. Heglind, R. Westergren, T. Niemi, M. Taittonen, J. Laine, N. J. Savisto, S. Enerback, and P. Nuutila. 2009. "Functional brown adipose tissue in healthy adults." *N Engl J Med* 360 (15):1518-25. doi: 10.1056/NEJMoa0808949.
Wang, Q. A., C. Tao, R. K. Gupta, and P. E. Scherer. 2013. "Tracking adipogenesis during white adipose tissue development, expansion and regeneration." *Nat Med* 19 (10):1338-44. doi: 10.1038/nm.3324.
Westerterp-Plantenga, M. S., S. G. Lemmens, and K. R. Westerterp. 2012. "Dietary protein - its role in satiety, energetics, weight loss and health." *Br J Nutr* 108 Suppl 2:S105-12. doi: 10.1017/s0007114512002589.
WHO. 2003. "Diet, nutrition and the prevention of chronic diseases." *World Health Organ Tech Rep Ser* 916:i-viii, 1-149, backcover.
WHO. 2015. "Obesity and overweight." World Health Organization, Accessed 11.05.15. http://www.who.int/mediacentre/factsheets/fs311/en/.
WHO. 2016. "Commission presents its final report, calling for high-level action to address major health challenge." World Health Organization, Accessed 03.16.16. http://www.who.int/end-childhood-obesity/news/launch-final-report/en/.
Williams, E. P., M. Mesidor, K. Winters, P. M. Dubbert, and S. B. Wyatt. 2015. "Overweight and Obesity: Prevalence, Consequences, and Causes of a Growing Public Health Problem." *Curr Obes Rep* 4 (3):363-70. doi: 10.1007/s13679-015-0169-4.
Wu, J., P. Bostrom, L. M. Sparks, L. Ye, J. H. Choi, A. H. Giang, M. Khandekar, K. A. Virtanen, P. Nuutila, G. Schaart, K. Huang, H. Tu, W. D. van Marken Lichtenbelt, J. Hoeks, S. Enerback, P. Schrauwen, and B. M. Spiegelman. 2012. "Beige adipocytes are a distinct type of thermogenic fat cell in mouse and human." *Cell* 150 (2):366-76. doi: 10.1016/j.cell.2012.05.016.
Wu, J., P. Cohen, and B. M. Spiegelman. 2013. "Adaptive thermogenesis in adipocytes: is beige the new brown?" *Genes Dev* 27 (3):234-50. doi: 10.1101/gad.211649.112.
Young, P., J. R. Arch, and M. Ashwell. 1984. "Brown adipose tissue in the parametrial fat pad of the mouse." *FEBS Lett* 167 (1):10-4.

APPENDIX

Appendix I – Diets

Table A.1. Diet compositions with analyzed nutrients

	Casein	Chicken	Cod	Pangasius
Analyzed				
Energy (kcal/100g)	580	580	570	570
Fat (g/100g)	24,9	23,7	24	23,8
Protein (g/100g)	39,8	39,6	40,6	39,5
Ingredients (g/100g)				
Casein	472			
Cod			482	
Chicken		501		
Pangasius				502
Sucrose	140	140	140	140
Fat from protein powder*	2,2	40,0	8,4	31,5
Corn oil (250g - fat from source)	248	210	242	219
Dextrin (Potato starch)	40,0	48,2	36,0	38,7
L-Cysteine	3	3	3	3
Cellulose	50	50	50	50
t-Butylhydroquinone	0,01	0,01	0,01	0,01
Mineral mix †	35	35	35	35
Vitamin mix ‡	10	10	10	10
Choline Bitartrate	2,5	2,5	2,5	2,5
Total (g)	1000,0	1000,0	1000,0	1000,0

* The calculated contribution of fat from protein sources. Calculation is based on data presented in table A.4.

Table A.2 Amino acid composition of the protein sources

	Casein	Chicken*	Cod *	Pangasius*
Amino Acid (mg/g)				
Indispensable				
Leucine	85,3	70,4	72,8	76,1
Isoleucine	43,7	40,7	40,3	43,6
Valine	59,4	43,9	46,3	46,8
Lysine	76,4	85,3	93,1	94,6
Methionine	25,0	24,7	28,3	27,7
Phenylalanine	44,8	34,9	34,6	38,1
Threonine	38,0	39,6	39,6	43,1
Tryptophan	11,0	10,3	9,5	9,9
Histidine	23,0	23,7	16,9	19,5
Dispensable				
Alanine	28,0	50,9	54,0	52,7
Arginine	30,7	53,8	53,7	56,9
Aspartate	70,6	89,0	101,8	101,0
Cysteine	0,36	1,02	1	0,95
Glutamate	213,1	135,2	146,9	148,3
Glycine	16,2	36,4	38,4	42,3
Proline	97,7	30,8	30,0	32,8
Serine	50,8	35,1	39,4	38,5
Tyrosine	45,9	28,9	30,0	31,5
Sum BCAA	188,4	155,0	159,3	166,5
Hydroxyproline	0,0	1,7	1,5	3,6
Taurine	0,0	0,6	4,8	2,6
Sum AA	949	824	871	896

* freezedried

Table A.3 Amino acid composition of the experimental diets

	Casein	Chicken	Cod	Pangasius
Amino Acid (mg/g)				
Indispensable				
Leucine	39,8	32,9	34,0	36,0
Isoleucine	21,2	19,6	18,7	21,1
Valine	28,5	21,2	21,5	22,7
Lysine	35,7	41,0	43,4	45,9
Methionine	13,3	12,6	14,5	14,0
Phenylalanine	21,1	15,7	16,1	17,6
Threonine	17,9	18,4	18,7	20,4
Tryptophan	4,9	4,9	4,5	5,0
Histidine	11,1	10,9	8,0	9,2
Dispensable				
Alanine	13,0	24,1	25,3	25,2
Arginine	14,7	24,7	25,3	26,8
Aspartate	32,6	42,7	47,8	48,8
Cysteine	5	8,4	8,6	8,5
Glutamate	96,4	64,7	69,4	69,9
Glycine	7,8	16,6	18,0	19,9
Proline	45,5	14,1	14,1	15,5
Serine	24,1	16,3	19,0	18,1
Tyrosine	20,9	12,7	13,8	14,4
Sum BCAA	89,5	73,6	74,3	79,8
Hydroxyproline	0,0	0,0	0,0	1,7
Taurine	0,00	0,25	2,37	1,23
Sum AA	444	388	410	427

Table A.4 Fatty acid composition of the protein sources

Fatty acids in neutral lipids				
	Casein	**Chicken***	**Cod ***	**Pangasius***
Fatty acid (mg/g)				
Sum SFA	0,52	18,10	21,70	20,30
Sum MUFA	0,51	27,20	18,70	19,90
18:1 (n-9)	0,46	22,57	6,88	18,16
Sum PUFA	0,48	14,10	58,50	8,70
18:2 (n-6)	0,44	11,75	1,15	5,31
20:4(n-6)	<0,01	0,32	2,09	0,68
Sum n-6	0,45	12,50	3,86	7,58
18:3 (n-3)	0,01	1,04	0,26	0,28
20:5(n-3)	<0,01	0,05	17,57	0,06
22:6 (n-3)	<0,01	0,09	33,99	0,21
Sum n-3	0,04	1,48	54,60	0,83
SUM FA	1,56	60,00	102,00	49,70
n-6/n-3 ratio	12,00	8,40	0,07	9,10
Fatty acids in phospholipids				
	Casein	**Chicken***	**Cod ***	**Pangasius***
Fatty acid (mg/g)				
Sum SFA	0,09	5,37	2,00	3,14
Sum MUFA	0,08	4,34	1,28	2,90
18:1 (n-9)	0,07	3,38	0,58	2,51
Sum PUFA	0,06	6,66	4,58	4,77
18:2 (n-6)	0,05	2,78	0,09	1,01
20:4(n-6)	<0,01	1,48	0,13	1,05
Sum n-6	0,05	5,06	0,26	3,87
18:3 (n-3)	<0,01	0,06	0,01	0,03
20:5(n-3)	<0,01	0,17	0,87	0,04
22:6 (n-3)	<0,01	0,82	3,24	0,44
Sum n-3	0,01	1,56	4,31	0,68
SUM FA	0,25	18,30	8,02	12,10
n-6/n-3 ratio	4,83	3,24	0,06	5,67

* freezedried

Table A.5 Fatty acid composition of the experimental diets

Fatty acids in neutral lipids				
	Casein	**Chicken**	**Cod**	**Pangasius**
Fatty acid (mg/g)				
Sum SFA	31,70	32,00	30,70	37,60
Sum MUFA	69,20	66,30	68,10	70,50
18:1 (n-9)	<0,01	62,40	65,42	67,63
Sum PUFA	134	111,00	130,00	113,00
18:2 (n-6)	131,58	108,40	124,80	111,52
20:4 (n-6)	<0,01	0,12	0,11	0,37
Sum n-6	132	109,00	125,00	113,00
18:3 (n-3)	2,02	2,04	2,04	0,03
20:5 (n-3)	<0.,01	0,03	0,95	0,04
22:6 (n-3)	<0.,01	0,04	1,73	0,11
Sum n-3	2,13	2,28	5,03	0,38
SUM FA	236,00	210,00	229,00	224,00
n-6/n-3 ratio	62,0	47,8	24,9	295,0
Fatty acids in phospholipids				
	Casein	**Chicken**	**Cod**	**Pangasius**
Fatty acid (mg/g)				
Sum SFA	0,29	3,05	1,32	1,78
Sum MUFA	0,59	2,76	1,28	2,12
18:1 (n-9)	0,56	2,17	0,86	1,89
Sum PUFA	1,09	4,89	3,69	3,62
18:2 (n-6)	1,07	2,65	1,08	2,06
20:4 (n-6)	<0,01	0,81	0,08	0,43
Sum n-6	1,07	3,88	1,20	3,22
18:3 (n-3)	0,02	0,05	0,03	0,04
20:5 (n-3)	<0,01	0,13	0,53	0,01
22:6 (n-3)	<0,01	0,53	1,85	0,18
Sum n-3	0,02	0,99	2,49	0,30
SUM FA	1,97	11,60	6,39	7,97
n-6/n-3 ratio	63,3	3,9	0,5	10,6

Appendix II – Histology

Table A.6 Reagents and time schedule for dehydration upon paraffin embedding

Reagent	Time (min)	Vendor
75% EtOH	45	Arcus Kjemi, Norway
95% EtOH	45 x 2	Arcus Kjemi, Norway
100% EtOH	45 x 3	Arcus Kjemi, Norway
Xylene	45 x 2	Prolabo
Paraffin	overnight	Histolab, Sweden
Paraffin	15	Histolab, Sweden

Table A.7 Reagents and time schedule for H&E staining

Reagent	Time	Vendor
Xylene	5 min	Prolabo
100 % EtOH	5 min	Arcus Kjemi, Norway
95 % EtOH	3 min	Arcus Kjemi, Norway
75 % EtOH	3 min	Arcus Kjemi, Norway
50 % EtOH	3 min	Arcus Kjemi, Norway
ddH2O	2 min	MilliQ Biocel, USA
Hematoxylin	30 sek	EMS
H2O (warm)	wash	
Eosin	15 sek	Sigma, USA
H2O	wash	
ddH2O	1 min	MilliQ Biocel, USA
50 % EtOH	1 min	Arcus Kjemi, Norway
75 % EtOH	1 min	Arcus Kjemi, Norway
95 % EtOH	1 min	Arcus Kjemi, Norway
100 % EtOH	5 min	Arcus Kjemi, Norway
Xylene	5 min	Prolabo

Appendix III - Immunohistochemistry

Table A.8 Time schedule for rehydration and rehydration

Reagent	Time	Vendor
Rehydration		
Xylene	15 min	Prolabo
96 % EtOH	15 min	Arcus Kjemi, Norway
75 % EtOH	15 min	Arcus Kjemi, Norway
50 % EtOH	15 min	Arcus Kjemi, Norway
ddH2O	15 min	MilliQ Biocel, USA
Dehydration		
50 % EtOH	5 min	Arcus Kjemi, Norway
75 % EtOH	5 min	Arcus Kjemi, Norway
96 % EtOH	5 min	Arcus Kjemi, Norway
100 % EtOH	wash	

Table A.9 Time schedule and reagents for immunohistochemistry

Reagent	Time	Contents and vendor
Citrate buffer (96 ^{0}C)	30 min	Tri-sodium citrate dehydrate + ddH2O
Cool down	20 min	
H2O	2 x 5 min	
3% H2O2 in MetOH	10 min	3 % H2O2 + MetOH (SIGMA)
1% Tween in PBS buffer	20 min	PBS + Technical Tween 20 (VWR)
PBS buffer	15 min	1000 ml ddH2O + 5 tablets Phosphate Buffered Saline (SIGMA)
Serum incubation	30 min	Vectastain, goat-normal serum (VECTOR laboratories)
Primary antibody	overnight	Anti UCP1 (C4/98), received from Prof Jan Kopecky and Dr. Pavel Flachs
PBS buffer	30 min	
Secondary antibody	1 hour	PBS buffer + Vectastain, anti-rabbit IgG antibody (VECTOR laboratories)
PBS buffer	30 min	
ABC	1 hour	PBS buffer + 2 drops vectastain ABC reagent A + 2 drops vectastain ABC reagent B + H2O2
PBS buffer	30 min	
DAB	7 min	5 ml ddH2O + 2 drops buffer stock + 4 drops DAB stock solution + 2 drops H2O2 solution
H2O	wash	
Hematoxylin	10 sek	EMS
H2O	wash	

Appendix IV – Ultra Sensitive Mouse Insulin ELISA Kit

Table A.10 Reagents in the Ultra Sensitive Mouse Insulin ELISA Kit

Product	Vendor
Anti-insulin antibody-coated microplate	Crystal Chem Inc., USA
Mouse insulin standard, lyophilised	
Anti-insulin enzyme conjugate stock solution	
Enzyme conjugate diluent	
Enzyme substrate (TMB) solution	
Enzyme reaction stop solution (1 N Sulfuric acid)	
Sample diluent	
Wash buffer stock solution	

Appendix V – RT-qPCR

Table A.11 Reagents and solutions used in RNA-purification

Reagent	Content	Vendor
Proteinase K Storage Buffer		Beckman Coulter, USA
Proteinase K soulution	Proteinase K + 8,4 ml Proteinase K Storage Buffer	Beckman Coulter, USA
Lysis Buffer Solution	600 µl Lysis Buffer + 30 µ Proteinase K	Beckman Coulter, USA
Binding Buffer (magnetic)		Beckman Coulter, USA
Wash- and Rebinding Buffer		Beckman Coulter, USA
70 % EtOH		Arcus Kjemi, Norway

Table A.12 RT-reaction mix

Reagent	Volume (µl)	Vendor
ddH2O	890	MilliQ Biocel, USA
10X TaqMan RT buffer	500	Applied Biosystems
25 mM MgCl2	1100	Applied Biosystems
10mM deoxyNTPs Mixture	1000	Applied Biosystems
50 µM Random hexamer	250	Applied Biosystems
RNase Inhibitor (20U/µl)	100	Applied Biosystems
Multiscribe Reverse Transcriptase	167	Applied Biosystems

Table A.13 Instrument setup for RT reaction

Step	Incubation	RT	Reverse Transcription Inactivation	End
	HOLD	HOLD	HOLD	HOLD
Temperature (^{0}C)	25	48	95	4
Time (min)	10	60	5	∞*
Volume (µl)	50			

Table A.14 Primers used for qPCR

Oligo name	**Sequence (5' to 3')**
Dgat1 forward	GGTGCCATCGTCTGCAAGA
Dgat1 reverse	CCACCAGGATGCCATACTTGA
Dio2 forward	GCCCAGCAAATGTAGAC
Dio2 rewerse	TGGCAATAAGGAGCTAGAA
Gpd1 forward	CTCATCACGACCTGCTATGG
Gpd1 rewerse	CTGCTCAATGGACTTTCCAG
Gyk forward	CAAATGCAAGCAGGACGATG
Gyk rewerse	GGCCCCAGCTTTCATTAGG
Ppargc1α forward	CATTTGATGCACTGACAGATGGA
Ppargc1α rewerse	CCGTCAGGCATGGAGGAA
Ucp1 forward	AGCCGGCTTAATGACTGGAG
Ucp1 reverse	TCTGTAGGCTGCCCAATGAAC

Appendix VI – Weight of liver, kidneys and *m. Tibialis anterior*

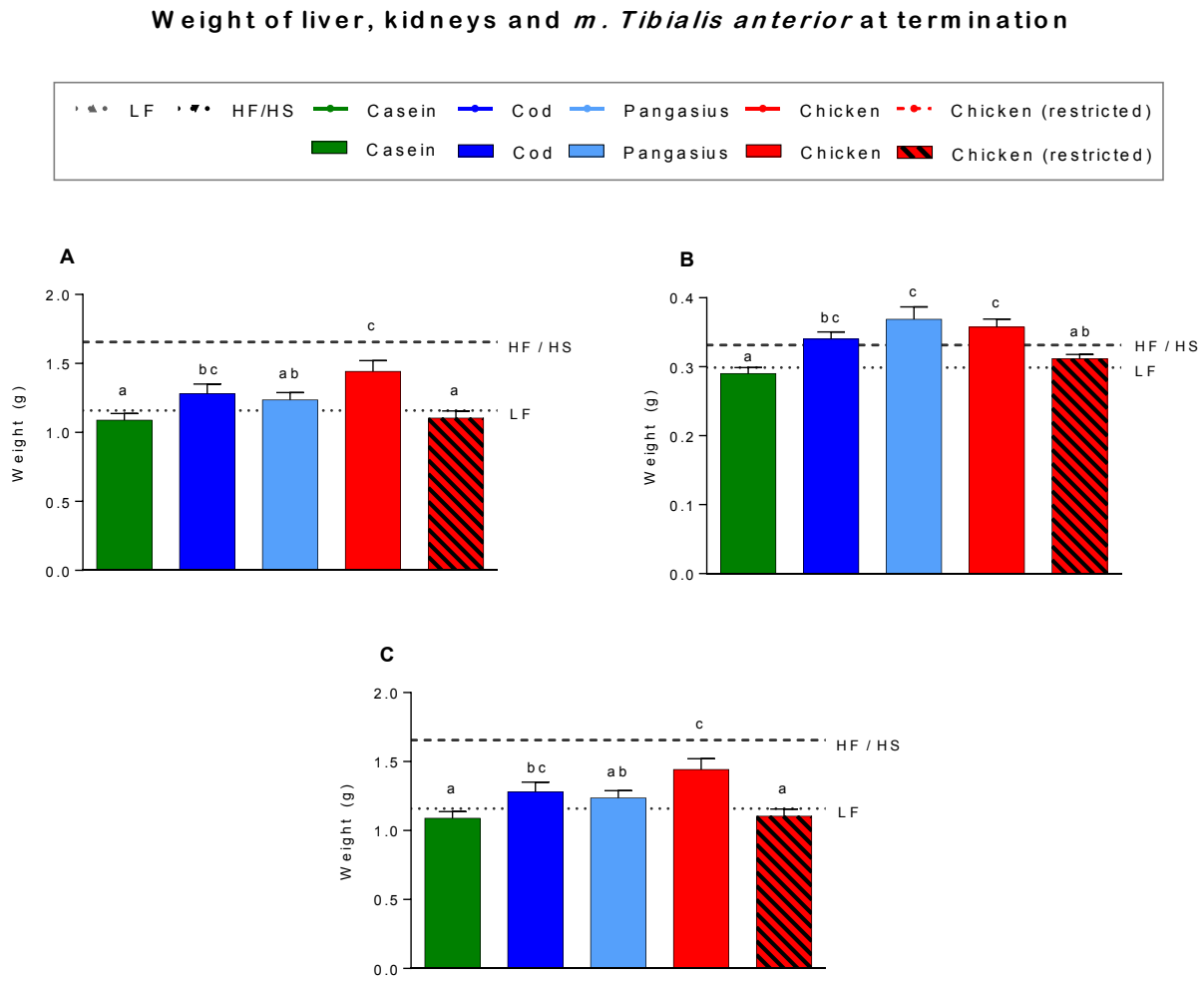

Figure A.1 Weight of liver, kidneys and *m. Tibialis anterior*. Weigt of liver (A), kidneys (B) and *m. Tibialis anterior* (C) at termination. All data were analyzed by one-way ANOVA with multiple comparison (uncorrected Fisher's LSD) of the mean of each experimental group. Results are presented as mean ± SEM. Statistical differences ($p \leq 0.05$) are marked by different letters.